



UNIVERSITÀ
DEGLI STUDI
DI PADOVA

UNIVERSITA' DEGLI STUDI DI PADOVA
Dipartimento di Ingegneria Industriale DII

Corso di Laurea Magistrale in Energy Engineering

Simulation and analysis of a district heating grid scenario
as part of a hybrid network

Relatore: Prof. Michele De Carli

Laura Vallese 2020215

Anno Accademico 2022/2023

Abstract

The heating sector in Germany accounts for more than half of the total energy consumption. Consequently, the decarbonization of this sector is crucial for reaching the GHG emissions reduction targets. In this context, district heating plays a fundamental role due to its high potential regarding the integration of renewable energy sources. An important opportunity is especially represented by hybrid networks, which consists of the coupling of generators, consumers and storage technologies belonging to different sectors.

The topic of this thesis is the development and simulation of a heat supply scenario including two hybrid grids for a district in the German town of Neuburg an der Donau. The heat is provided by two district heating systems with decentralized storage tanks, which are supported by sector coupling technologies such as electric heating elements and heat pumps. The electricity surplus generated by rooftop photovoltaic plants is exploited for feeding these coupling technologies, through a supply-oriented approach. The PV power that is not consumed by these technologies is used to partially run a large HP that supplies one of the two considered DHGs.

The results of the yearly simulation, carried out in the software MATLAB Simulink, are compared to a reference scenario without sector coupling and with a similar scenario analyzed in a previous work: the main difference is in the supply of the new development area, that in this thesis is provided by a low temperature district heating grid, supplied by a groundwater heat pump.

The results show that the analyzed energy route has the potential to be an exemplary solution for other similar districts. The use of the efficient heat pump technology for the supply of the new development area represents an opportunity to further implement sector coupling.

However, the scenario requires further investigation to improve some critical issues. The storage concept for the new development area could be revised, so that heat losses are reduced and the system is optimized. Moreover, the issue regarding high GHG emissions due to the presence of the central heat pump has to be addressed, for example by planning the installation of a ground photovoltaic plant next to the district.

Keywords: District heating, Hybrid networks, Sector coupling, Power-to-heat, Smart thermal grids.

Riassunto esteso

Il settore del riscaldamento in Germania rappresenta più della metà del consumo totale di energia. Di conseguenza, la decarbonizzazione di questo settore è fondamentale per raggiungere gli obiettivi di riduzione delle emissioni di gas serra. In questo contesto il teleriscaldamento ha un ruolo fondamentale, grazie al suo elevato potenziale di integrazione delle fonti energetiche rinnovabili. Un'importante opportunità è rappresentata soprattutto dalle reti ibride, che consistono nell'accoppiamento di generatori, utenze e tecnologie di accumulo appartenenti a settori energetici diversi.

L'argomento di questa tesi consiste nello sviluppo e nella simulazione di uno scenario di fornitura di calore da parte di reti ibride per un quartiere della città tedesca di Neuburg an der Donau. Il calore è fornito da due reti di teleriscaldamento con serbatoi di accumulo decentralizzati, supportati da resistenze elettriche e pompe di calore che permettono di realizzare il *sector coupling* fra il sistema elettrico e il settore del riscaldamento. La potenza elettrica eccedente generata dagli impianti fotovoltaici, installati sui tetti degli edifici residenziali, viene sfruttata per alimentare questi componenti, attraverso un approccio *supply-oriented*. L'energia fotovoltaica che non viene consumata da queste tecnologie viene utilizzata parzialmente per il funzionamento della pompa di calore centrale che alimenta una delle due reti di teleriscaldamento considerate.

I risultati della simulazione annuale, effettuata con il software MATLAB Simulink, sono confrontati con uno scenario di riferimento senza *sector coupling* e con uno scenario simile analizzato in una tesi precedente: la differenza principale è nell'alimentazione della nuova area residenziale, che in questa tesi è fornita da una rete di teleriscaldamento a bassa temperatura, alimentata da una pompa di calore ad acqua di falda.

I risultati mostrano che lo scenario analizzato ha il potenziale per diventare una soluzione esemplare per altri quartieri simili. L'utilizzo dell'efficiente tecnologia della pompa di calore per l'approvvigionamento della nuova area residenziale rappresenta un'opportunità per implementare ulteriormente il *sector coupling*.

Tuttavia, lo scenario richiede ulteriori approfondimenti, in modo che alcuni aspetti critici possano essere migliorati. L'accumulo decentralizzato per la nuova area residenziale potrebbe essere rivisto, in modo da diminuire le perdite nella rete e ottimizzare il sistema considerato. Inoltre, la questione riguardante le elevate emissioni di gas serra dovute alla presenza della pompa di calore centrale deve essere affrontata, ad esempio pianificando l'installazione di un impianto fotovoltaico sui terreni disponibili nelle vicinanze del quartiere.

Table of Contents

Abstract.....	II
Riassunto esteso.....	III
List of figures.....	VI
List of tables.....	VIII
List of abbreviations.....	IX
1 Introduction.....	1
1.1 Background.....	1
1.2 Classification of the work.....	4
1.3 Objective of the thesis.....	5
2 Fundamentals for the heat supply.....	6
2.1 Introduction to District Heating.....	6
2.2 Hybrid networks.....	9
3 Heat supply scenario for the Heckenweg district.....	11
3.1 General information on the district.....	11
3.2 Energy routes for heat supply.....	12
3.3 Analyzed energy route.....	15
3.3.1 Heat supply concept.....	15
3.3.2 Decentralized storage concept.....	16
4 Design of the district heating grids and of the components.....	18
4.1 Heating and domestic hot water requirement.....	18
4.2 Pipes.....	19
4.3 Pumps.....	22
4.4 Central heat pump.....	23
4.5 Groundwater system.....	24
4.5.1 Data regarding the aquifer.....	24
4.5.2 Required groundwater flow.....	25
4.6 Central and decentralized storages.....	26
4.6.1 Electric elements.....	27
4.6.2 Decentralized heat pumps.....	28
5 Simulation model.....	30
5.1 Software description.....	30
5.2 Model development.....	31
5.2.1 Central heat pump.....	32
5.2.2 Central storage.....	33

5.2.3	Control strategy for central heat pump and storage tank	34
5.2.4	Decentralized storage tanks	35
5.2.5	Models for the grids.....	40
6	Simulation results	43
6.1	Photovoltaic surplus and heat demand.....	43
6.2	Usage of the sector coupling technologies	44
6.3	Energy supplied by the district heating grids and heat losses.....	45
6.4	Pump energy.....	48
6.5	Primary energy.....	50
6.6	Greenhouse gas emissions	51
7	Conclusion and outlook	55
	Literature	X
	Appendix	XIV
A.1	Heat load and heating demand.....	XIV
A.2	Other parameters for the buildings.....	XVI

List of figures

Figure 1.1 World total GHG emissions from fuel combustion per product [1].	1
Figure 1.2 Overview of the German heating sector [4].	2
Figure 1.3 Total energy consumption by end use in the German residential sector [4].	3
Figure 1.4 Possible transition path for heat supply of buildings in the European Union, according to the Heat Roadmap Europe project [9].	4
Figure 2.1 Development and timeline of the district heating technology [14].	7
Figure 2.2 Timeline for the district heating generations [9].	7
Figure 3.1 The Heckenweg district in Neuburg an der Donau.	11
Figure 3.2 Energy routes proposed in the project context [11].	14
Figure 3.3 First energy route proposed for the district.	14
Figure 3.4 Scheme of the energy route that is analyzed in this work.	17
Figure 4.1 Pipeline scheme: the different paths are identified with numbers.	20
Figure 4.2 Characteristic curves of the grid pump for the new development area [34].	22
Figure 4.3 Characteristic curves of the grid pump for the existing buildings area [34].	23
Figure 4.4 Temperature of groundwater in Neuburg an der Donau along the year 2022 [37].	24
Figure 4.5 Groundwater mass flow rate in a site nearby the Heckenweg district [38].	25
Figure 4.6 HPDL (left) and ÜPDL (right) storage tanks from the company ENERPIPE [43].	27
Figure 4.7 Storage concept, version with electric element [12].	28
Figure 5.1 Basic THB block, with overview of the parameters that are carried by the signal [47].	30
Figure 5.2 Modified heat pump block from the CARNOT library [49].	32
Figure 5.3 Type 1 Storage block from the CARNOT library [49].	33
Figure 5.4 Input and output heights in the central storage (measures in mm).	34
Figure 5.5 Input and output heights in the storage, heights are referred to the tanks for the existing buildings [12].	35
Figure 5.6 Model for the decentralized storage equipped with internal heat exchanger (HPDL) [49].	36
Figure 5.7 Model for the decentralized storage equipped with external heat exchanger (ÜPDL) [49].	37
Figure 5.8 Representation of a house connection with supply pipe (red), return pipe (blue), flow diverter and flow mixer blocks (from the model created for the DHG for the new development area) [49].	41
Figure 6.1 Monthly PV surplus, heating demand and DHW demand for the Heckenweg district.	43
Figure 6.2 Shares of heat supply for the second energy route.	44
Figure 6.3 Comparison of the shares of electricity for sector coupling in the two energy routes.	45
Figure 6.4 Duration curves of the different scenarios.	46
Figure 6.5 Comparison between the two DHGs operated in the second energy route, regarding final energy supplied and heat losses of the grid.	47
Figure 6.6 Final energy supplied and heat losses of the grid, comparison among the different scenarios.	47
Figure 6.7 Monthly values for the final energy delivered by the DHG and correspondent heat losses for the second energy route.	48
Figure 6.8 Shares of energy supplied by the two DHGs and of the energy required by the grids' pumps for the second energy route.	49

Figure 6.9 Pump energy demands and the savings of the sector coupling energy-routes with respect to the reference scenario.	49
Figure 6.10 Primary energy for the different heat supply scenarios.	51
Figure 6.11 CO2 emissions for every scenario.	52
Figure 6.12 The available area that could be exploited for the installation of a ground PV plant [55] is highlighted in red.....	53
Figure 6.13 GHG emissions in case the HP for the second energy route was completely supplied by PV power, and savings with respect to the reference case.	53

List of tables

Table 4.1 Dimensioning of the pipeline for the new development area.	21
Table 4.2 Dimensioning of the pipeline for the existing buildings area.	21
Table 4.3 Main features of the central heat pump [35].	23
Table 5.1 Developed Simulink models.	32
Table 5.2 Threshold temperature for the control of the central storage tank's charging.	34
Table 5.3 Threshold temperature for the control of the decentralized storage tanks' charging...	38
Table 5.4 Threshold temperatures considered in the control strategy for the heating element charging. Values that were considered for the existing buildings in the previous thesis are crossed out.	39
Table 5.5 Main features of the two DHGs.	41
Table 6.1 PEF values for the different considered sources [52], [53].	50
Table 6.2 CO ₂ equivalent values for the different sources [53].	52
Table A.1 Heat load and heating demand for the buildings in the Heckenweg district.	XIV
Table A.2 Other considered parameters for the buildings in the Heckenweg district.	XVI

List of abbreviations

5GDHG	Fifth Generation of District Heating and Cooling
BHE	Borehole Heat Exchanger
CARNOT	Conventional And Renewable eNergy systems Optimization Toolbox
CDH	Cold District Heating
CHP	Combined Heat and Power
COP	Coefficient Of Performance
DFH	Double-Family House
DH	District Heating
DHG	District Heating Grid
DHW	Domestic Hot Water
GHG	Greenhouse Gases
GCHP	Ground Coupled Heat Pump
GWHP	Ground Water Heat Pump
HP	Heat Pump
HPLD	<i>Hochleistungsspeicher mit Dezentrale Ladung</i>
HVAC	Heating Ventilation Air Conditioning
IEA	International Energy Agency
LTDH	Low Temperature District Heating
LTDHC	Low Temperature District Heating and Cooling
MFH	Multi-Family House
PEF	Primary Energy Factor
PV	Photovoltaic
RES	Renewable Energy Sources
RH	Row House
SFH	Single-Family House
SWHP	Surface Water Heat Pump
SWND	<i>Stadtwerke Neuburg an der Donau</i>
THB	Thermohydraulic Bus
ÜPDL	<i>Übergabespeicher mit Dezentrale Ladung</i>
VDEW	<i>Verband der Ernährungswirtschaft</i>

1 Introduction

1.1 Background

Climate change is one of the biggest challenges for the World: greenhouse gases (GHG) emissions have continued to increase up to 2019, with only a small drop in 2020 mainly caused by the Covid pandemic (Figure 1.1) [1].

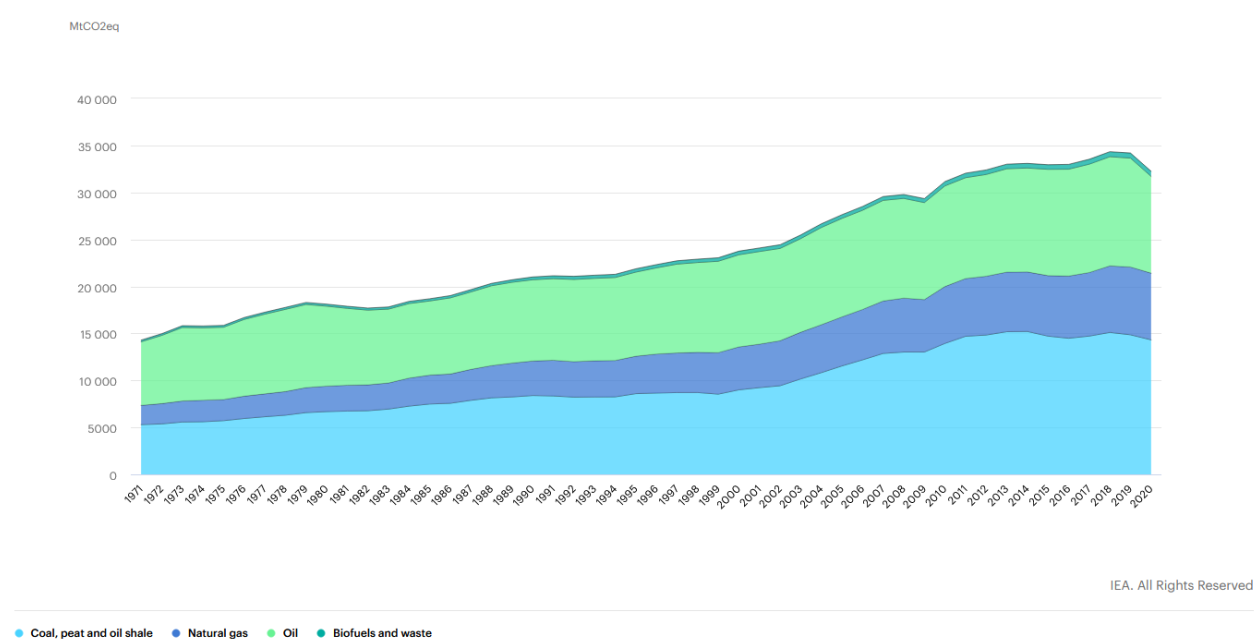


Figure 1.1 World total GHG emissions from fuel combustion per product [1].

A much bigger effort is required for reducing them, particularly with reference to the Paris agreement [2], whose aim is to limit global warming to 1.5 °C with respect to pre-industrial levels. Fossil fuels, the major contributors to energy-related emissions, should be phased out, leaving room for renewable energy sources (RES) integration.

In addition to the international agreements, most of the countries have pledged to follow plans for energy transition. In particular, a focus on Germany is presented in the following, since this thesis is focused on a district heating (DH) system located in a German town. The Climate Change Act (June 2021) has set a target of at least 88% GHG emissions reduction by 2040 and GHG neutrality by 2045. Moreover, the act includes targets regarding primary energy consumption: the goal is to reduce them by 30% by 2030, and to halve them by 2050 [3].

In 2020 the German heating sector (without considering cooling) accounted for about 55% of the total energy consumption: consequently, it plays a fundamental role in achieving decarbonization goals. In Figure 1.2, data from IEA [4] show that almost 50% of the German heating sector still exploited natural gas, while the share of waste and renewables had increased up to about 30%. The shares of oil and coal had decreased a lot, but coal was still relevant, with a share of more than 20%.

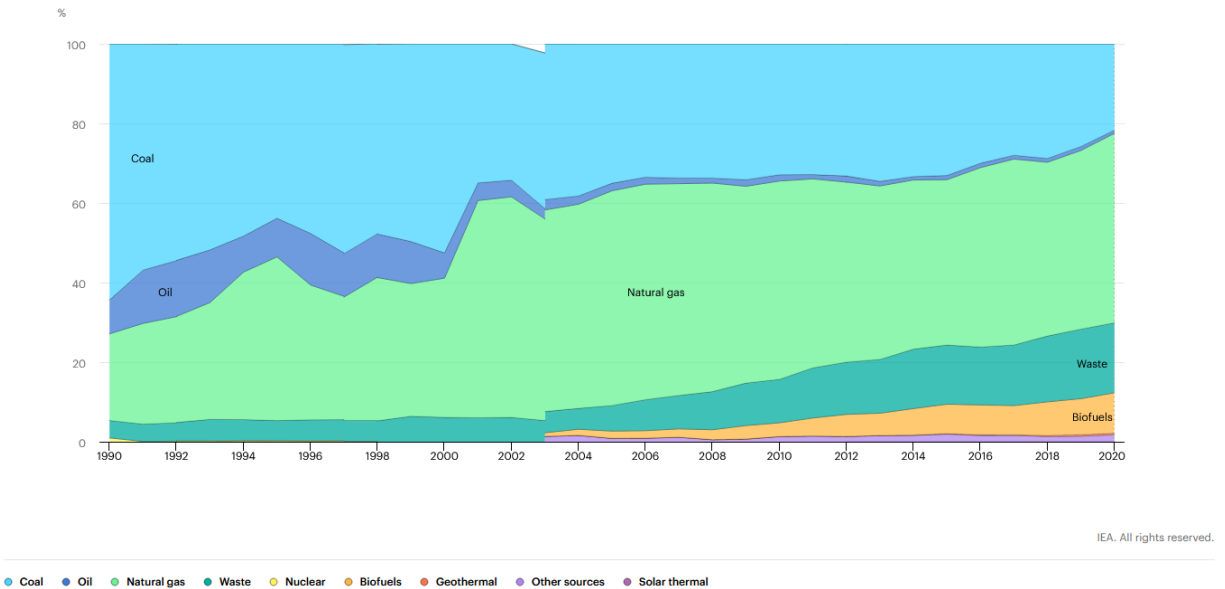


Figure 1.2 Overview of the German heating sector [4].

The relevance of the heating sector is even more evident if residential is taken into account: in 2020, it accounted for about 90% of the final energy consumption in buildings [5]; this is particularly highlighted in Figure 1.3, reporting data from IEA [4]. The aforementioned Climate Change Act provides a target of 68% GHG emissions reduction in the building sector by 2030 [3].

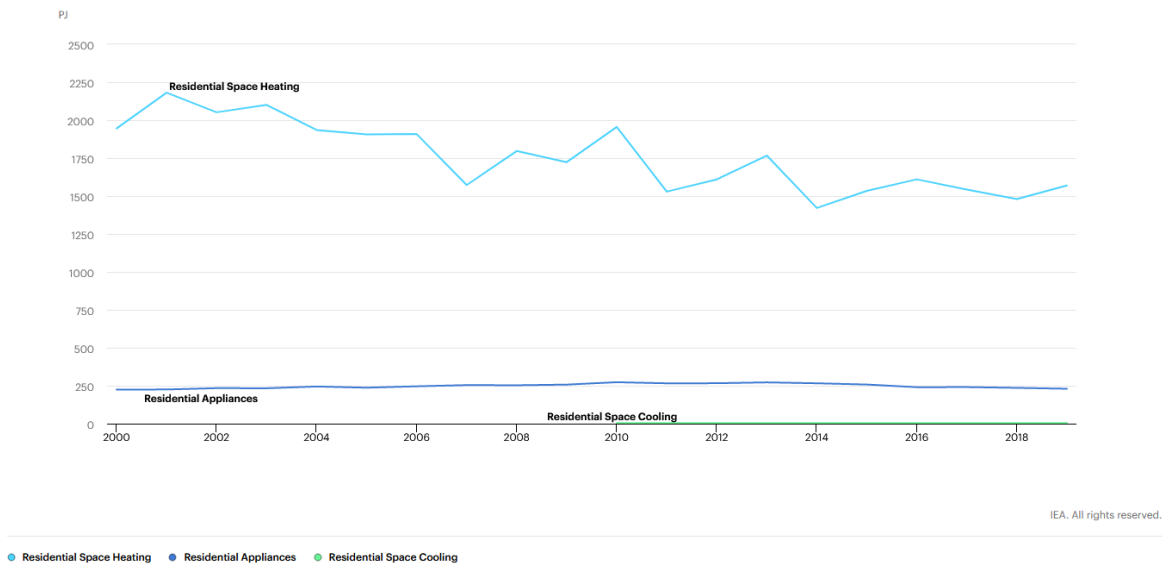


Figure 1.3 Total energy consumption by end use in the German residential sector [4].

New generation district heating is a key technology for helping the decarbonization of the heating sector: in Germany, district heating grids (DHG) cover 14% of the buildings’ space heating demand [6], [7], [8]. However, a deep transformation and improvement can be further implemented, since 86% of the heat is provided to them by CHP plants, 85% of which are fueled by coal or gas [7], [8]. German policies regarding DH focus on exploitation of decentralized energy sources and of heat pumps driven by excess electricity [6].

On a broader level, today DH meets 13% of EU heat demand and 8% of the World demand [9]. A possible transition path from the current heat supply for EU, including exploitation of DH, is represented in Figure 1.4.

Regarding GHG emissions, targets for Europe are set by the European Climate Act: it aims for 55% reduction by 2030 and to neutrality by 2050, mainly achievable through compensation of residual emissions with processes that remove GHG from atmosphere. Furthermore, the Renewable Energy Sources Directive has the target of 32% increase of RES by 2030, while the European Green Deal aims to improve energy efficiency and building refurbishment, increase RES utilization and develop an integrated, networked and digitalised energy market [3]. Decarbonization of the heating sector is of major importance for Europe as well: heating and cooling of buildings accounts for 50% of the final energy consumption and 25% of GHG emissions, that are expected to grow up to 80% in 2050 [10].

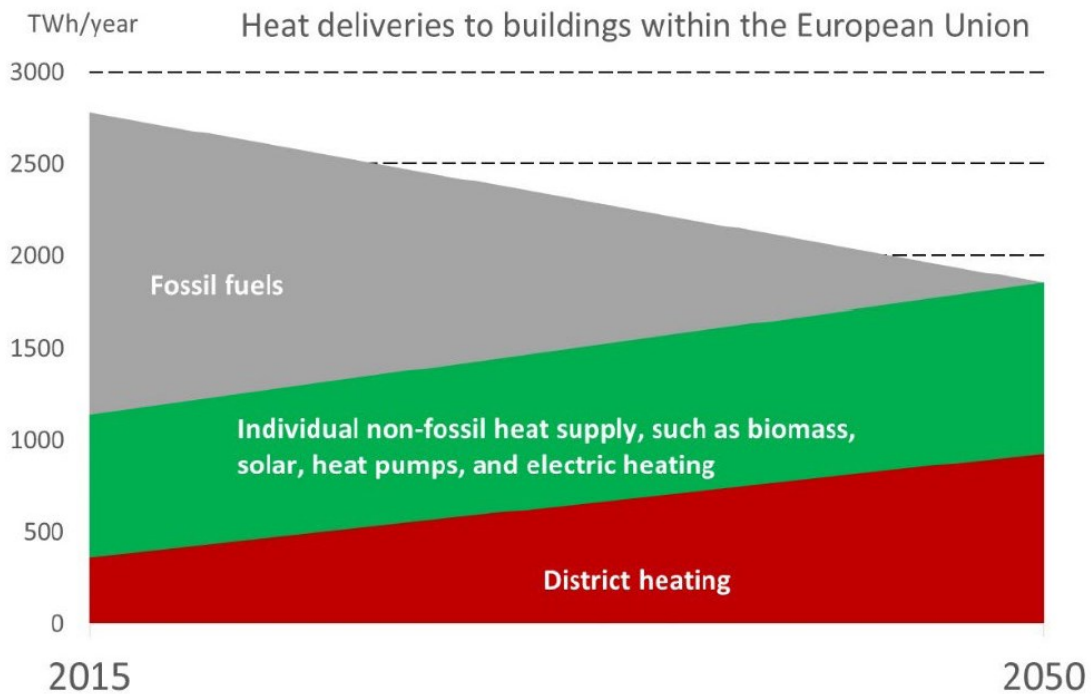


Figure 1.4 Possible transition path for heat supply of buildings in the European Union, according to the Heat Roadmap Europe project [9].

1.2 Classification of the work

This thesis is related to the German project HybridBOT_FW, whose main objective is the transformation, optimization and flexibilization of district heating grids, through the implementation of hybrid energy networks [11]. Particular attention is paid to the development of a supply-oriented operation, regarding the heat and electricity sectors. Information about hybrid networks can be found in 2.2.

The case study that is considered in the project involves the German city of Neuburg an der Donau: the description of the considered district is presented in detail in 3.1.

The project involves different partners, such as the company ENERPIPE and the *Stadtwerke* (municipal utilities) of Neuburg an der Donau (SWND). The thesis' work is part of the Fraunhofer IEE (Institute for Energy Economics and Energy System Technology) work package AP2, that has the main objective of developing a co-simulation model regarding local sector coupling, thus evaluating the interaction between the electricity network and the heating sector.

1.3 Objective of the thesis

The objective of the work is to evaluate the primary energy, GHG emissions and heat losses of a heat supply scenario (called energy route) proposed for the DHG to be developed for a neighbourhood of a German town. The focus is on the implementation of a hybrid network through power-to-heat coupling technologies, especially considering exploitation of PV power through a supply-oriented perspective. This is done by connecting the decentralized storages with sector coupling components, such as electric elements and heat pumps, able to exploit the PV generated surplus.

The evaluation is carried out through the analysis of the results obtained from a dynamic thermal simulation, performed in the time frame of one year. The results are only related to the thermal grid, and therefore the efficiencies of the coupling technologies are not taken into account. The results are then compared with the ones obtained for another energy route analyzed in a previous thesis [12] and for a reference scenario in which sector coupling is not implemented.

Before the creation of the model, the main components of the grid are carefully designed: this allows to build a consistent model that can be used as base for successive implementation in reality.

2 Fundamentals for the heat supply

2.1 Introduction to District Heating

District heating is a local networked system that can be used for supplying thermal energy from a central source to the buildings of a neighborhood or of a city [13]. The network consists of pipes, where a suitable distribution medium flows.

There are different types of configurations that can be chosen for a district heating grid [14]. The traditional design consists of a radial network, where the pipes have different lengths depending on how far the consumer is from the supply point: this could lead to insufficient available differential pressure for the consumers that are furthest away from the supply. To avoid this problem, usually a ring configuration is adopted, so that every consumer has an equal pipe length. Moreover, this type of grid allows to increase flexibility, with the possibility of expanding the network and integrating different supply points.

The development of the DH technology can be followed through different steps, correspondent to different historical periods and improved technical features (Figure 2.1 and Figure 2.2). The first grid was commercialized in the USA in 1877: the transport fluid was steam, characterized by a higher heat capacity with respect to water [15]. This first generation DH required a large diameter supply pipe and a small diameter condensing return pipe, made of concrete. This kind of system was developed in order to substitute boilers located in the apartments [13], and is affected by relevant disadvantages: heat losses, accidents, return pipe corrosion and low energy efficiency [15]. Even if this technology is now outdated, these kinds of systems are still used in New York and in Paris, due to their favorable residential density. The second generation, implemented from 1930, exploited pressurized water with supply temperature higher than 100°C, that flowed in insulated pipes. It was largely exploited in the former URSS, but without heat demand control; in other countries the quality of these systems was better, and they are still present in some parts of water based DHG systems. This technology was mainly developed for promoting CHP exploitation [13]. Starting from 1970s, it was possible to reduce supply temperature to a value between 80°C and 100°C, using prefabricated and pre-insulated metal pipes. This third generation is highly spread in Nordic countries and is still used today: the main reason behind its deployment refers to the need of ensuring security of supply and energy efficiency, after the two oil crisis happened [13]. The first three generations represent the Warm District Heating (WDH) grids: heat is supplied from different plants and can satisfy users' demand without requiring additional heat supply.

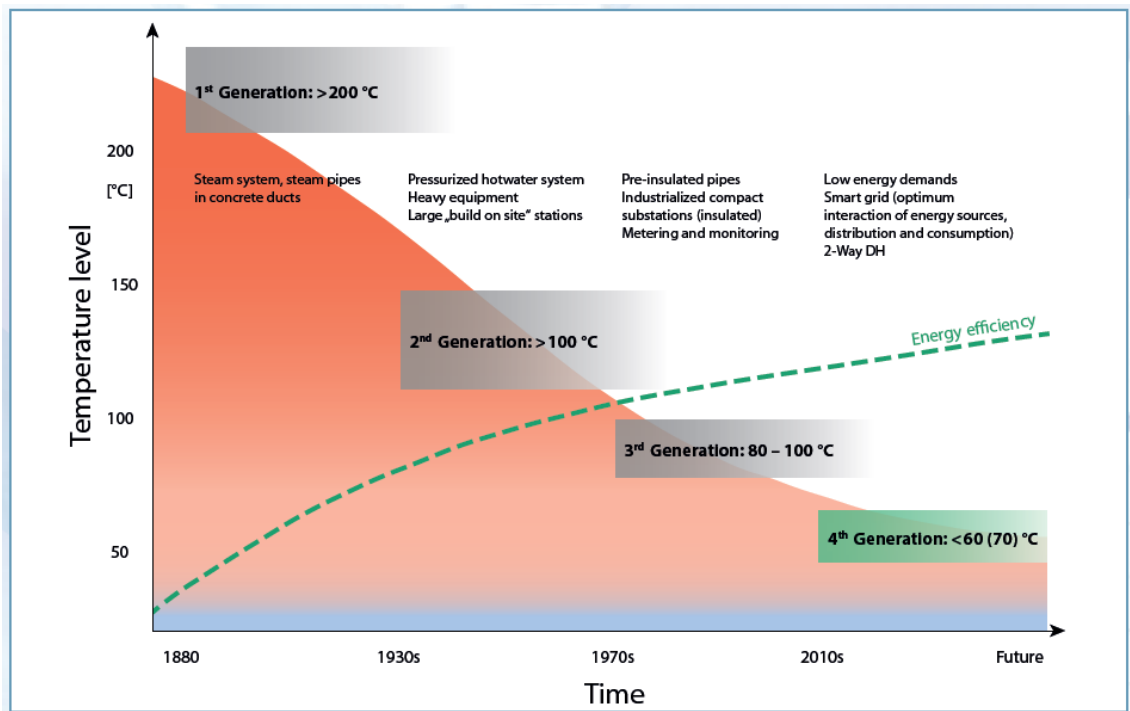


Figure 2.1 Development and timeline of the district heating technology [14].

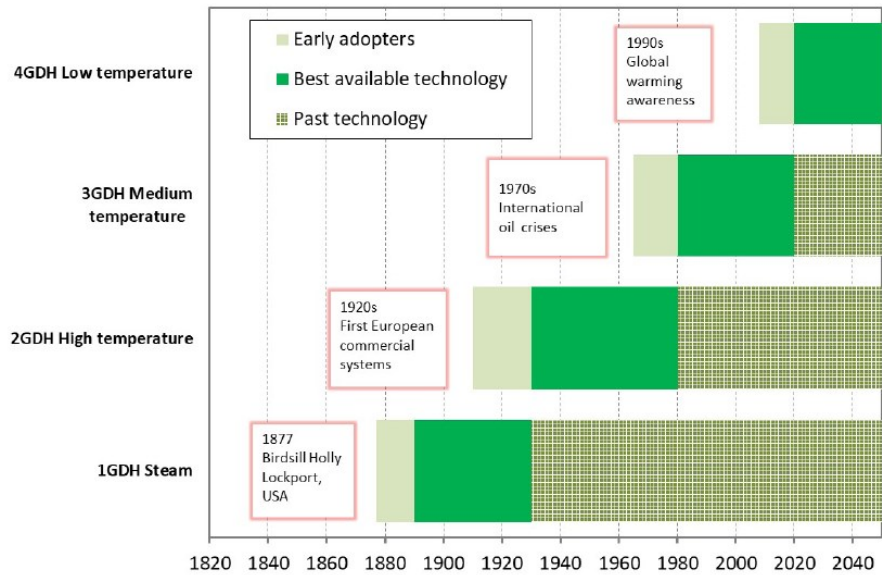


Figure 2.2 Timeline for the district heating generations [9].

The fourth generation, also referred to as low temperature district heating (LTDH), is currently being developed: exploiting a supply temperature lower than 70°C leads to several advantages, both from distribution and generation point of view. Regarding distribution, benefits involve lower losses, a better quality match between supply and demand, decreased thermal stress and scalding risk, use of plastic pipes instead of steel ones; as for generation, lower supply temperatures lead to an increase in the CHP plants power-to-heat ratio and in the waste heat recovered through flue gas condensation, a higher heat pumps' COP (coefficient of performance), an increase in the heat demand capacity, and an increased utilization of low-temperature waste heat and renewable energy. The possibility of integration of small-scale decentralized heat sources is a very important aspect, that also allows the possibility of prosumer exploitation if a bidirectional flow is considered: in fact, these systems are particularly suitable for domestic users, mostly passive or low energy houses. The ideal terminal unit for LTDH is floor heating, even if radiators and convectors could be exploited for some applications. The main disadvantages related to LTDH are the necessity of fault detection in substations, the Legionella development risk for domestic hot water (DHW) supply, the high specific capital costs in low heat density areas and the challenge regarding existing buildings, that typically require higher heating supply temperatures. Regarding the last point, energy efficiency interventions are crucial for allowing the decrease of heat demand, and consequently a better exploitation of LTDH. The sources that are usually exploited are solar collectors, heat pumps (also geothermal), combined heat-and-power (CHP) plants or excess heat from industry. It is important to consider that lots of CHP plants are currently fueled by coal or gas: for allowing the decarbonization of the heating sector, a transition towards biomass and waste supply for these plants should be implemented, even if this would lead to a lower contribution of CHP technology in DH. An important challenge regarding LTDH is digitalization by means of sensors, and automated recording, transfer and storage of data: this would allow to optimize the efficient use of connected infrastructures, generate scheduling according to forecast demand and enhance renewable integration [9], [14].

Recently, a new generation has been introduced, even if a unified and clear definition has not been agreed: [16] mainly highlight that 5th generation district heating and cooling (5GDHC) differs from the previous one because of bidirectionality, that allows simultaneous distribution of heating and cooling with the same pipes to different buildings, and the possibility to exploit excess thermal energy from chillers. The development of this technology promotes the adoption of a "Transactive energy" business process, sustained by a consumer/prosumer-centric approach. In literature, this technology is also called LTDHC (low temperature district heating and cooling), CDH (cold district

heating) or energy networks (energy is the component of a form of energy that cannot be converted into exergy).

2.2 Hybrid networks

A hybrid energy network can be defined as “a local optimized connection of different energy grids” [17]. This concept is strictly related to sector coupling, that consists in linking the electricity, heat and transport sector: the energy provided by one sector is used in another one and can be converted again. The main purposes are the increase of efficiency and flexibility and the exploitation of low carbon electricity to decarbonize other sectors. This work focuses on power-to-heat, that is the implementation of heat generation through renewable electricity integration [18].

The electrification of the heating systems, and particularly of DHG, can be direct or indirect. Heat pumps and electric boilers are the key technologies for direct electrification, that is the focus of this thesis. In the case of indirect electrification, excess heat from electric-driven industrial processes and from electrofuel production is taken into account [17].

One of the most important advantages of sector coupling implementation is the possibility to exploit temporary renewable surplus generation [19]: however, it should be taken into account that power-to-heat contribution to decarbonization is possible if the decrease of emissions due to fossil fuels substitution in the heating field is higher than the potential emission increase due to additional electricity demand. Moreover, an aspect to pay attention to is the fact that yearly demand profiles for heating and electricity are different: the electricity profile is quite constant, while the heating demand is higher during the winter months (DHW has a more constant behaviour) [20]. In this context, the behaviour of households can also be decisive for emission savings: optimal use of heat pumps should be carried out [19].

Residual load is another key concept to be taken into account: if the energy demand is higher than the electricity generated by RES (negative residual load), importing from other countries is the best solution [21], prioritizing RES generated electricity. However, an increase in the electricity demand would have an impact on infrastructures and operation [18], and this should not be neglected. A solution for overcoming RES fluctuations and increasing flexibility is demand side management, that focuses on electricity-based heat generators, such as heat pumps combined with thermal storages [6], [21], [22]. This type of management implies decreasing the loads and re-scheduling on-off times for the user systems [15].

An easier development of hybrid energy networks can be carried on by considering LTDH: in fact, heat pumps are a key technology that works as interface (or coupling point) between the electricity and the heating sectors. For example, decentralized heat pumps working with PV can use the DHG return temperature for domestic hot water (DHW) preparation, so that part of the return mass flow is cooled by the heat pump, leading to an increase in the network efficiency [9]. Another possible coupling point to the electricity network are electric boilers [23]: in particular, the lower efficiency of electric boilers allows a larger integration of the variable RES [17]. However, since heat pumps' COP is higher, they are a better solution for longer, more frequent and lower RES surpluses; on the other hand electric boilers should be preferred for shorter, rarer and higher RES surpluses [18]. Another study also pointed out that an increase in RES generation leads to an increase in the utilization of heat pumps, while determining a decrease in CHP plants' operation [24].

A very relevant aspect regarding not only hybrid networks, but LTDH grids too, is the opportunity to limit biomass dependence [13]: this is an important issue because of the increased competition between transport and green chemicals sectors [25]. Most importantly, biomass is a limited resource that is not able to replace the entire fossil fuel share used today, especially if long term is considered [26]. [27] analysed the case of a 100% renewable city in Denmark, and pointed out that the system should be able to work without decreasing the opportunity of a total renewable supply for other areas: this implies to reduce biomass usage. Results from [17] show that both increasing electric boiler and HP capacity contribute to a reduction of the biomass consumption, with HP capacity being more effective.

3 Heat supply scenario for the Heckenweg district

3.1 General information on the district

The Heckenweg district considered in the project is in Neuburg an der Donau, a town located in Bavaria, in Germany. The project focuses on four different areas, mainly including residential buildings: one existing buildings area, two new development areas and an area with three commercial buildings (energy provider, kindergarten and nursery). Both single- and multi-family buildings are located in the district; the former are either detached or semi-detached (double-family) houses. In this thesis, that refers to the first part of the project, the 33 buildings of the existing area and the 25 buildings of the first new development area are considered, as highlighted in Figure 3.1.



Figure 3.1 The Heckenweg district in Neuburg an der Donau.

The existing houses were built in different time frames between 1940 and 2003, while the buildings of the new development area have not been built yet. The construction is scheduled for 2025, and consequently some assumptions must be made in the project context.

Two different district heating grids operated by SWND are already present in the town. The first one (called A4) is used to provide process heat at high temperature (120°C) for energy-intensive industries (e.g. glass processing), and is supplied by a combined heat and power (CHP) plant fed by natural gas, together with a gas boiler for peak coverage. The supply for the second existing grid (H5) consists of waste heat recovered from the CHP flue gases; the temperature (90 °C) is especially suitable to provide heating and DHW to residential buildings. A constant operation mode is applied to both grids, implying that the supply temperature does not change with the outdoor temperature [28].

The new district heating grids that are going to be implemented in the Heckenweg district are exclusively designed with the purpose of supplying space heating and domestic hot water, thus neglecting potential summer cooling requirements.

3.2 Energy routes for heat supply

In the HybridBOT project context, three different energy routes were identified: these consist of scenarios characterized by different supply concepts that include sector coupling implementation. This thesis focuses on the modelling and simulation of one of them, as well as on the analysis of relevant results, such as primary energy consumption, heat losses and CO₂ emission.

In each proposed scenario, the “old” area is supplied by the existing district heating network H5, which is operated in sliding-constant mode: this means that the supply temperature is kept to 80°C during the coldest months and is decreased up to a minimum value (70°C or 75°C depending on the case) in the warmest months. This allows the grid to adapt to the fluctuating demand while reducing distribution heat losses, that increase with the temperature difference between the district heating fluid and the surrounding (the ground). The minimum value adopted in the warm months is based on the necessity to supply DHW at a temperature level high enough to avoid hygiene problems: the minimum temperature required is equal to 60 °C. A purely variable operation mode is not suitable for DHW supply, due to the risk to reach a too low temperature, that could cause Legionella growth [28].

The reference temperature that is considered is the so called allocation temperature, that is a geometric average of the outdoor temperature over a long time period: this is a better choice with

respect to considering the actual outdoor temperature, since it could lead to too high fluctuations on the grid supply temperature [29].

On the other hand, the new development area can be supplied either by H5 (first option) or by a new grid through a central heat pump (second and third option). The third proposed option further implements a central solar thermal plant, that could be exploited for supporting Domestic Hot Water (DHW) preparation and satisfy part of the storage demand, especially during summer operation. Since summer cooling is not performed, the solar plant could also be exploited for ground regeneration purposes, if a GCHP (ground coupled heat pump) with BHEs (borehole heat exchangers) is included as central heat generator.

In all the considered concepts, each residential unit is connected to a thermal buffer storage, that is charged by the district heating grid through a heat exchanger and is able to provide both heating and DHW: storage is important for flexibility, to cover peak loads and to ensure the security of supply [30].

For implementing sector coupling in the grid, every tank is equipped either with electric elements or with air-water heat pumps, with the purpose of reheating. An electric element consists of a resistance that heats up when the electric current flows through it, as described by Joule's first law (3.1).

$$P = R \cdot I^2 [W], \quad (3.1)$$

where P is the heating power, R is the electric resistance [Ω] and I is the electric current [A].

Thus, it is a simple and cheap solution, but the efficiency is much lower with respect to heat pumps. Air-water HPs are able to exploit air as a source for the refrigerant vapor compression cycle, that provides heat at the higher temperature level required by the supply.

The electricity required by the sector coupling components is provided by decentralized rooftop photovoltaic (PV) plants, one for each building, and the generated excess is then used for running the central HP supplying the new development area. The electrical efficiency of the coupling technologies is not investigated nor taken into account in this work.

A picture describing the main features of the different scenarios is shown in Figure 3.2.

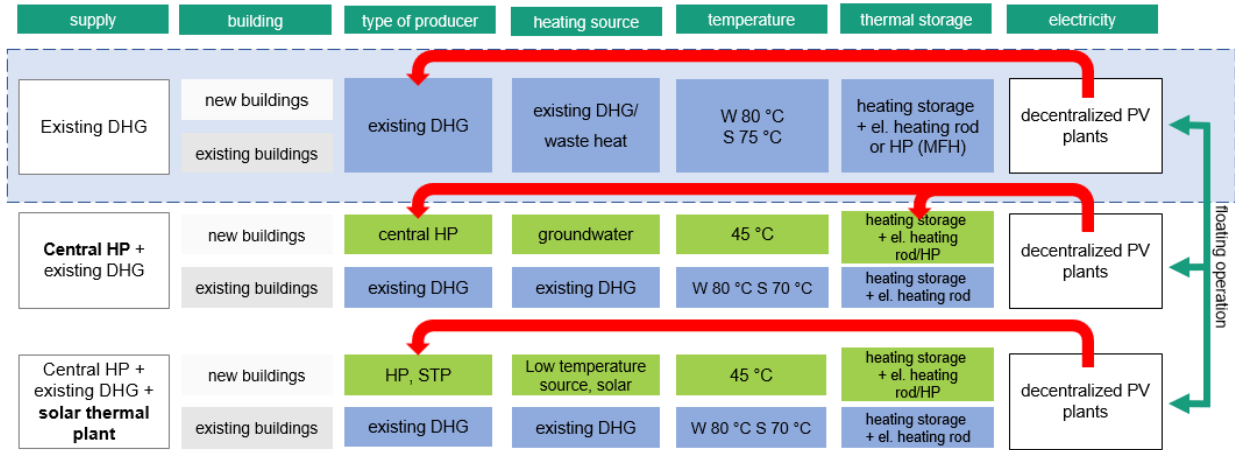


Figure 3.2 Energy routes proposed in the project context [11].

The first energy route, represented in Figure 3.3, was analyzed in a previous Master's thesis [12], where it was also compared to a reference scenario without sector coupling. This thesis is the continuation of that work.

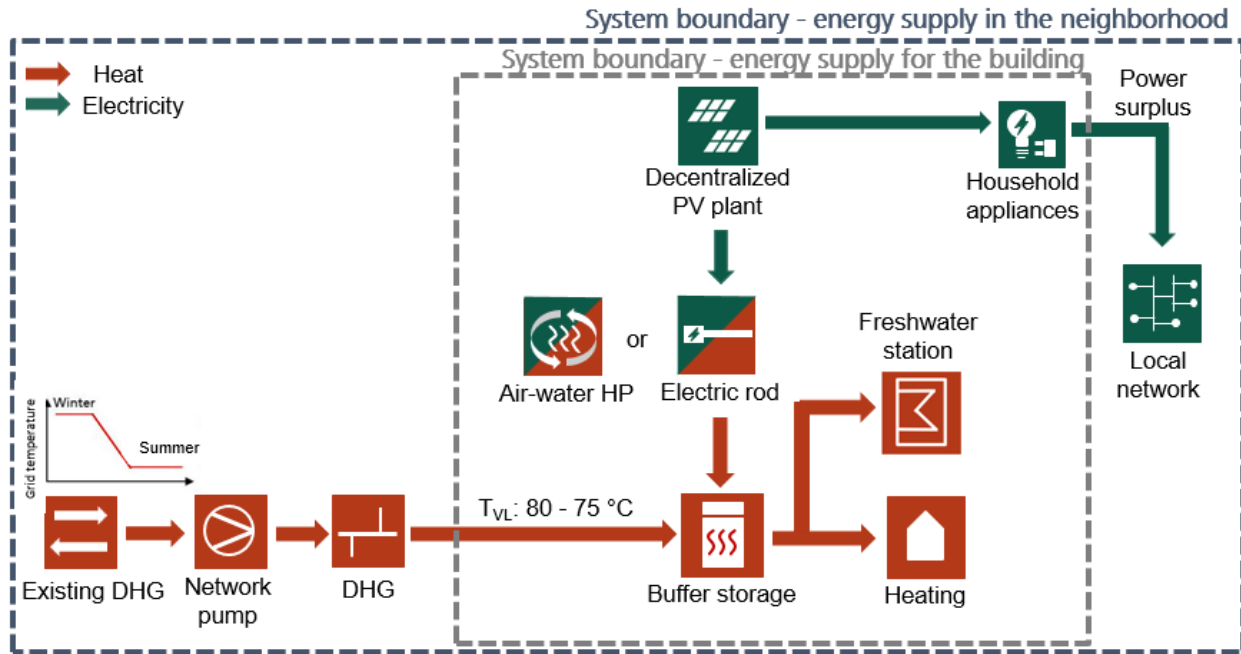


Figure 3.3 First energy route proposed for the district.

3.3 Analyzed energy route

3.3.1 Heat supply concept

The energy route that is analyzed in this thesis is the second one that is shown in Figure 3.2: the exploitation of a central heat pump allows to lower the supply temperature from 80 °C to 45 °C, with all the benefits related to LTDH (listed in 2.1), and represents a further sector coupling technology. The temperature difference between supply and return is set to 15 K.

This heat supply concept can only be applied to the new development area, since the heating terminal units for these buildings are going to be radiant floor systems: in fact, these require inlet temperatures in the range 28-35 °C, way lower than the requirement for traditional radiators (60-70 °C). The concept could be applied to the existing buildings area only by including temperature boosting technologies, such as heat pumps or solar thermal collectors [14].

The best supply option for an efficient central HP operation would be a local heat source with almost constant temperature: this mainly leads to the choice among a GCHP with BHEs, a GWHP (groundwater heat pump) or a SWHP (surface water heat pump).

A GCHP was the initial choice to be taken into account in the project context. However, a first dimensioning made with the ASHRAE method resulted in a large number of BHEs (around 300), meaning that high drilling costs would have been required. Moreover, the ground regeneration problem must be faced if the HP is only exploited for heating purposes, especially if a large system is considered. Due to these issues, an alternative supply source had to be identified. A GWHP with water reinjection was finally considered to supply the new buildings area. This option was chosen after having considered the following aspects:

- The required drilling is much less than what is required for a big GCHP: only one extraction well and one injection well are necessary. Sufficient distance between the two wells is needed: however, this is not calculated in the thesis, since this aspect is not relevant for the software simulation.
- The geographical area is suitable for this type of system [31].
- This system can be “replicated” for other similar towns in an easier way. For example, a system exploiting river water could be suitable for this case, given the proximity of the Donau river; however, it cannot be implemented in areas far from watercourses.
- The ground regeneration issue is not relevant in the case of groundwater exploitation, especially if reinjection is planned.

A more detailed description of the GWHP system is provided in 4.5.

The electricity required by the GWHP is expected to be supplied by the PV power that exceeds the buildings' electricity demand and the supply of the coupling technologies connected to the decentralized storages. If this residual PV is not sufficient, the central HP is going to be supplied partially by the electric grid.

A big buffer storage is also included as interface between the central HP and the DHG, to hydraulically separate the two parts and to allow the supply at the desired temperature.

The heat supply concept for the existing buildings area is the same as in the first scenario. The grid is going to be connected to the existing H5 through a head station, that allows the new section to be hydraulically separated by the existing one.

The two areas of the Heckenweg district are thus going to be supplied by two different grids. For this reason, a new dimensioning of the pipelines and of the grid pumps is required, together with the choice of an adequate central HP for the new development area.

In contrast with the energy route considered in the previous work [12], this scenario does not involve the switch off of the two district heating grids during summer operation. This choice was made because the two separated grids are smaller than the one considered in the previous work, and consequently the heat losses are less relevant; regarding the new development area, this choice is also related to the lower supply temperature of the system, that implies further heat losses reduction. In any case, PV potential is enhanced during summer due to the higher solar radiation and is consequently primarily exploited thanks to the control strategy that is implemented for electric elements and decentralized heat pumps.

3.3.2 Decentralized storage concept

The decentralized buffer storage concept is essentially the same for all the energy routes: tanks connected to single- or double-family houses are equipped with an electric element, while this last is substituted by air-water heat pumps in big multi-family buildings. These choices are made because heating elements are a less expensive technology with respect to heat pumps, but the latter are more suitable for MFH connections due to the higher efficiency and to the high heat demand required by this kind of buildings.

Decentralized PV plants are used for feeding these sector coupling technologies by following a supply-oriented approach and allow reducing the heat that has to be supplied by the DH system. Thus, the implemented charging control strategy for these components has the purpose to take advantage of the available PV surplus as much as possible.

To ensure hygiene, the DHW supply is supposed to be hydraulically separated from the tank through a freshwater station; however, this last component is not taken into account in the model. More information about the choice and design of the storages is described in 4.6.

The final concept for this energy route is represented in Figure 3.4:

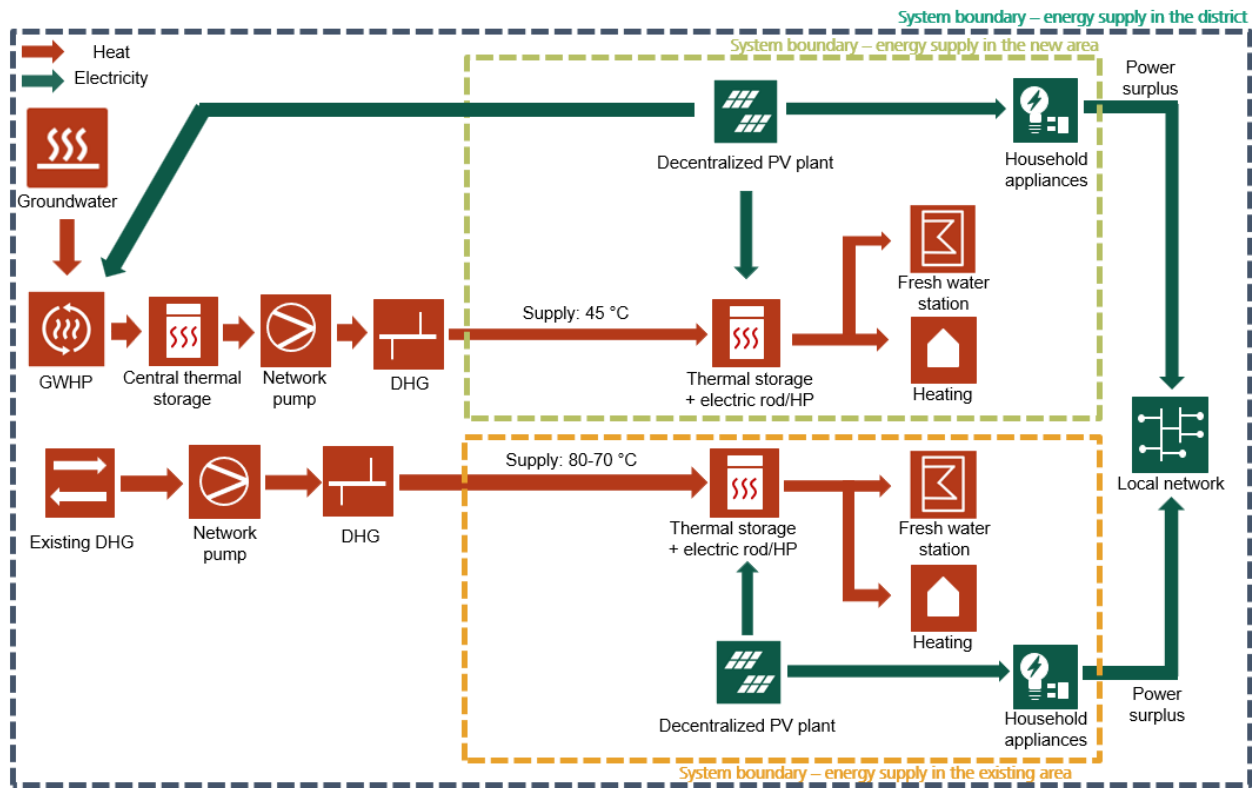


Figure 3.4 Scheme of the energy route that is analyzed in this work.

4 Design of the district heating grids and of the components

The design of the main components of the system is presented in this chapter. This step is fundamental in general to develop an efficient system and in particular in this case to ensure that the simulation model is as consistent as possible.

The design of the DHGs, as well as of the components such as HPs and storage tanks, is carried out by considering the maximum heat load occurring on the most critical day in winter, so that security of supply is ensured. Thus, heat load and demand (both for heating and DHW) are required as inputs and have to be evaluated before starting the sizing. Since the heating load is lower than the design value for most of the year, the grid and the components work mostly at partial load (< 50% of the design load).

All the design procedures are carried out by considering adequate standards and technical handbooks. After sizing, the components are chosen from datasheets and catalogues, so that the model can be used as basis for implementation in reality.

4.1 Heating and domestic hot water requirement

The data regarding heating load and demand was already available and is shown in Table A.1.

These values were calculated in the project context [12], based on specific values per square meter of heated area, provided by SWND. They are based on natural gas demand measurements for different types of buildings in the town: this is the best approximation that can be considered, since there is no information regarding actual energy consumption in the past years. The energy standards for the different buildings are considered as well: in the case of the new buildings, an assumption had to be made. A room temperature of 20 °C was taken into account.

Data about the DHW demand were available as well but had to be calculated again due to SWND's choice to change the input data with respect to the previous work: a reference value of 23 L/(s·person) was taken into account to represent the withdrawal per person. Then, the withdrawal for each building was obtained by multiplying the specific value for the number of people that are living in the building: estimates of 3.5 people in a SFH and 2 people per residential unit in double- and MFH were considered. This led to the consideration of much less DHW load with respect to what was considered in the previous thesis.

The DHW profiles were generated by using the software DHWcalc, developed by the University of Kassel [32]: the draw-offs are distributed throughout the year based on a probability function, with a timestep that in this work was set to 15 minutes.

After obtaining the profiles, the DHW requirement for each withdrawal was calculated through (4.1):

$$\dot{Q}_{DHW} = \dot{m}_{DHW} \cdot c_{p,w} \cdot \Delta T_{DHW} [W], \quad (4.1)$$

where \dot{m}_{DHW} [kg/s] is the withdrawn mass flow rate, $c_{p,w}$ [J/kg·K] is the specific heat of water, ΔT_{DHW} [K] is the temperature difference between the hot and cold water in the DHW circuit.

4.2 Pipes

The dimensioning of the district grid's pipeline is done by considering appropriate guidelines [28], and the calculations are made by using an Excel sheet programmed with Macros.

The diameters of the pipes are chosen depending on the specific pressure drop per meter of pipe length: the maximum value must be in the range 250 – 300 Pa/m, but the range 150 – 200 Pa/m must be taken into account when the critical node is considered. The critical node is usually identified as the district heating line that connects the heat supply to the most distant customer. As stated before, since two grids are considered, different dimensioning for the new and the existing areas must be made. The scheme of the pipelines is represented in Figure 4.1.

For each section of the scheme, the following procedure [28] has been followed:

- Volume flow rate calculation according to (4.2), depending on the maximum heat load and on the temperature difference in the grid. For the existing site, cautious peak load values have been considered.

$$\dot{V}_{max} = \frac{\dot{Q}_{max}}{\rho_w \cdot c_{p,w} \cdot \Delta T_{s-r}} [m^3/s], \quad (4.2)$$

where \dot{Q}_{max} [W] is the maximum heat load, ρ_w [kg/m³] is water density, $c_{p,w}$ [J/kg·K] is the specific heat of water, ΔT_{s-r} [K] is the grid temperature difference between the supply and return.



Figure 4.1 Pipeline scheme: the different paths are identified with numbers.

- Length determination for each section, considering both supply and return: this values were mostly already available [12]. A new 10 m pipe is considered for the supply of the existing buildings district, as can be seen from Figure 4.1.
- Pipe diameter determination, based on diagrams dependent on heat load and temperature difference.
- Actual flow velocity calculation:

$$u = \frac{4 \cdot \dot{V}_{max}}{\pi \cdot D^2} [m/s], \quad (4.3)$$

where \dot{V}_{max} [m³/s] is the volume flow rate calculated in (3.2), D [m] is the pipe diameter.

- Actual specific pressure drop calculation, as in (4.4). This is made up of two components: the friction pressure loss in straight section and the local pressure loss due to pipe fittings (elbows, junctions, etc.).

$$\Delta p = \rho_w \cdot \frac{u^2}{2} \cdot \left(\frac{\lambda \cdot L}{D} + \sum \zeta_i \right) [Pa/m], \quad (4.4)$$

where ρ_w [kg/m³] is water density, u [m/s] is the flow velocity, λ [-] is the pipe friction coefficient, L [m] is the pipe length, D [m] is the pipe diameter, ζ_i [-] is the characteristic coefficient for localized pressure losses, dependent on the type of material.

Table 4.1 and Table 4.2 show the results of the dimensioning of the pipelines for the two areas:

Table 4.1 Dimensioning of the pipeline for the new development area.

Path nr.	Heating Load [kW]	Volume flow rate [m ³ /h]	Pipe diameter [m]	Max flow speed [m/s]	Pipelines pressure difference [Pa/m]	Pipe length [m]
51	100	2.91	32	0.795	175.5	101
6	60	1.75	32	0.477	71.8	85
7	188	5.48	50	0.667	77.9	206
8	288	8.39	50	1.021	199.3	88
9	521	15.18	65	1.128	177.3	510
101	22	0.64	20	0.481	137.3	33
98	808	23.54	80	1.537	296	10

Table 4.2 Dimensioning of the pipeline for the existing buildings area.

Path nr.	Heating Load [kW]	Volume flow rate [m ³ /h]	Pipe diameter [m]	Max flow speed [m/s]	Pipelines pressure difference [Pa/m]	Pipe length [m]
1	634.7	36.69	100	1.131	92.1	145
2	91.5	5.29	40	1.0657	268.2	175
31	543.2	31.40	100	0.968	70.1	103
32	68.2	3.94	40	0.794	160.1	131
4	14.0	0.81	25	0.384	76.9	21
5	28.6	1.65	32	0.450	71.8	101
10	17.4	1.01	25	0.479	113.2	33

As in [12], composite pipes with plastic sheathing are considered: they belong to the Insulation Series 2 of the company LOGSTOR [33].

4.3 Pumps

The choice of the pump for each considered DHG is done depending on the required pump head:

$$H = \frac{\Delta p_{CN} + \Delta p_{HC}}{\rho_w \cdot g} \quad [m], \quad (4.5)$$

where Δp_{CN} is the pressure drop in the critical node of the grid [Pa], Δp_{HC} is the pressure difference that is required above the house connection of the least favorable customer [Pa], ρ_w [kg/m³] is water density, g [m/s²] is gravity acceleration.

The differential pressure difference to be applied by the pump in the new site is equal to 2.01 bar, with a corresponding head of 20.61 m. Regarding the existing site, the values are respectively 0.87 bar and 9.023 m.

The pumps are chosen by using the software Wilo-Select 4 [34], that requires the volume flow, the differential pressure difference and the head of the pump as inputs.

For the new area, the pump Atmos GIGA-B 32/125-4/2 is selected: the characteristic curves are shown in Figure 4.2.

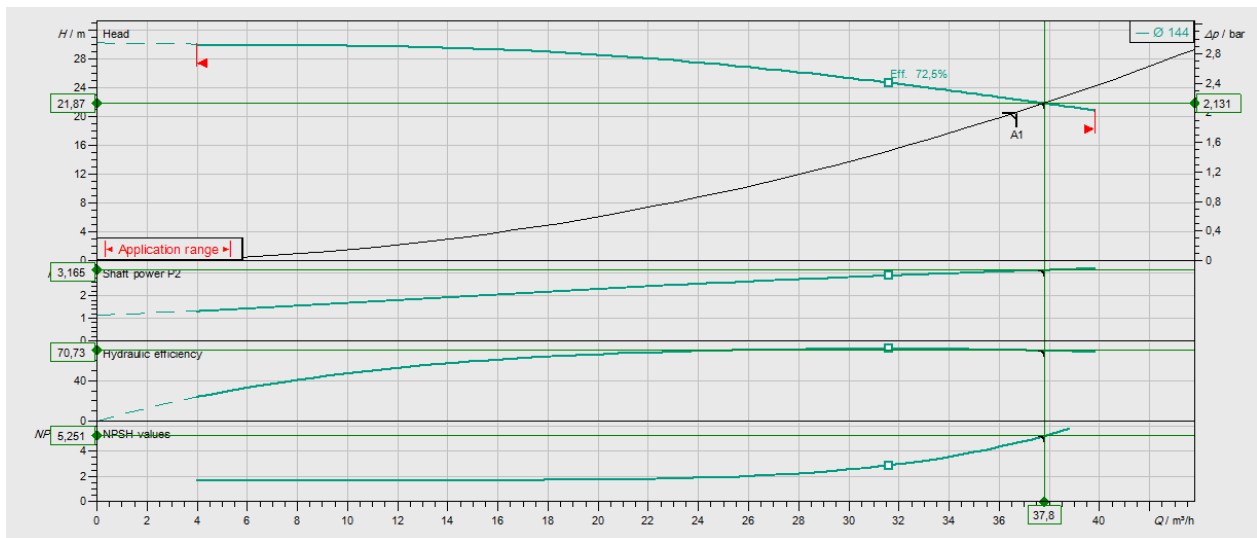


Figure 4.2 Characteristic curves of the grid pump for the new development area [34].

For the existing area, the pump Atmos GIGA-B 32/85-1,1/2 is chosen: the characteristic curves are shown in Figure 4.3.

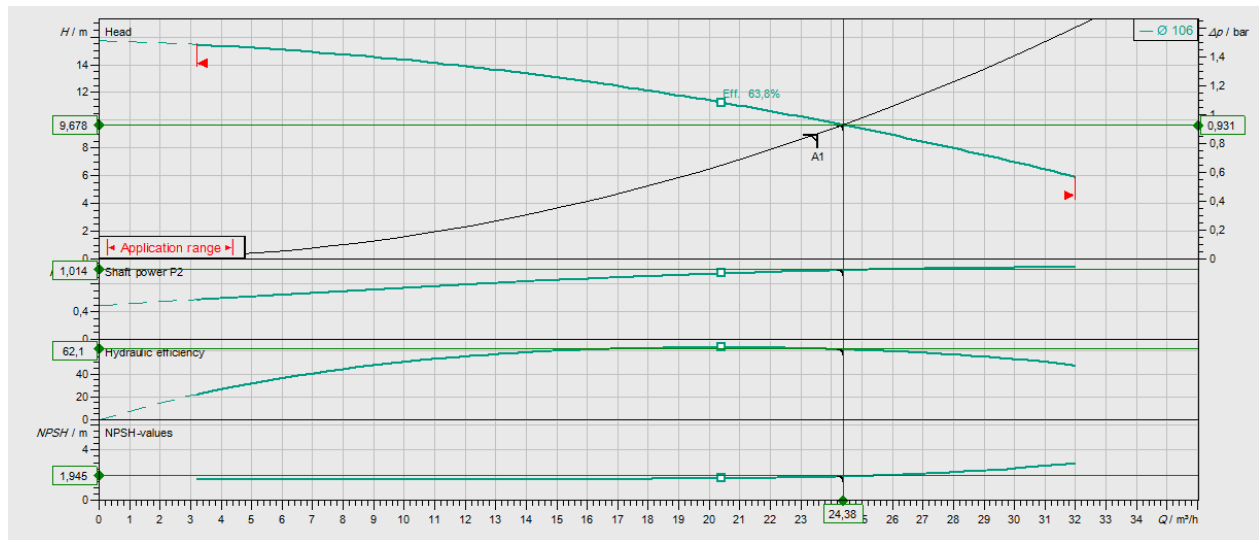


Figure 4.3 Characteristic curves of the grid pump for the existing buildings area [34].

Since pressure is not evaluated in the simulation, pumps are not included in the model. However, the final results will also evaluate their electricity consumption.

4.4 Central heat pump

The central heat pump that supplies the new development area is chosen by considering the total heat load required by the buildings, that is almost 635 kW. A water/water HP from the company HiRef [35] is chosen, considering a source temperature equal to 10 °C and supply temperature of 45 °C. The data about the considered model is summarized in Table 4.3.

Table 4.3 Main features of the central heat pump [35].

Model	Heating capacity	COP
HiRef 30XSW576WS_F5	675 kW	4.31

4.5 Groundwater system

4.5.1 Data regarding the aquifer

The upper groundwater layer in Neuburg an der Donau is located at an average depth of about 2.7 m under the surface [36]. The temperature of the water, considering the year 2022, oscillates between 8.4 °C and 11.8 °C [37], as shown in Figure 4.4.

Temperature of springs from 01.01.2022 to 31.12.2022

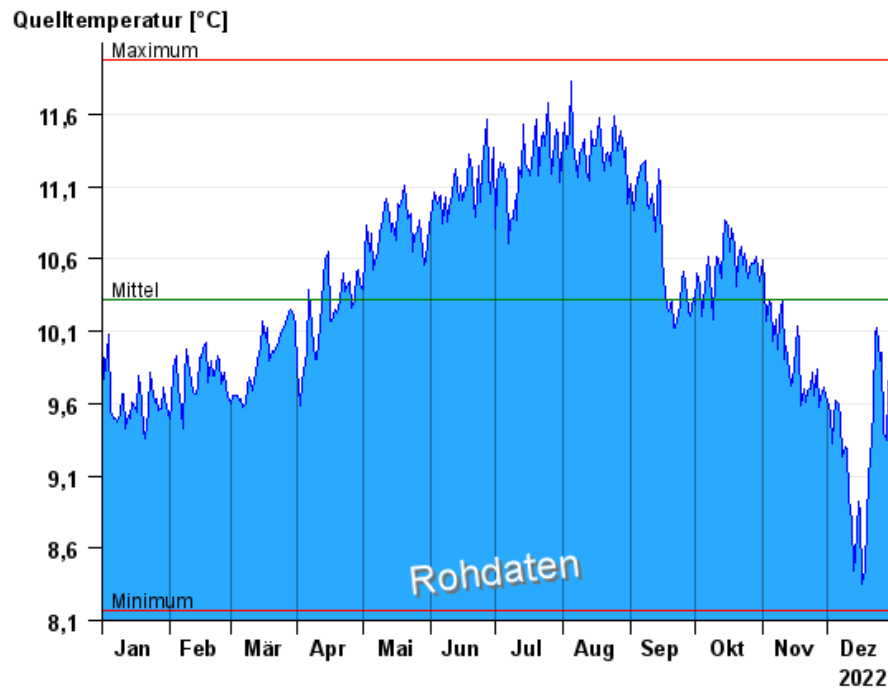


Figure 4.4 Temperature of groundwater in Neuburg an der Donau along the year 2022 [37].

Figure 4.5 shows that the mass flow rate of the well oscillates between circa 75 L/s and 125 L/s [38].

Ground level [m above sealevel]: 360.00

Messstelle: Karstquelle Ettling

Nr: 11507

Grundwasserleiter: Weißer Jura / Malmkarst

Zeitraum: Mai 2022 - Apr 2023

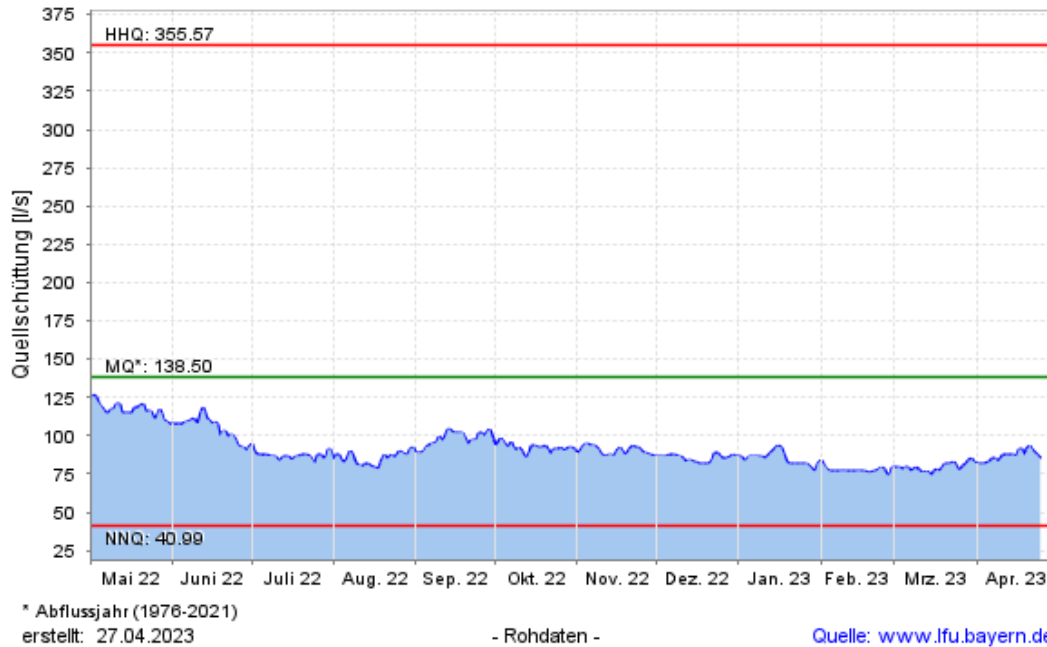


Figure 4.5 Groundwater mass flow rate in a site nearby the Heckenweg district [38].

4.5.2 Required groundwater flow

The groundwater flow required for the energy demand of the new buildings district is calculated according to Blázquez et al. [39], by considering (4.6).

$$F_h = \frac{L_h}{4.18 \times (T_i - T_{oh})} \cdot \frac{(COP - 1)}{COP} [L/s], \quad (4.6)$$

where L_h [kW] is the net heating load of the new development area, T_i [°C] is the groundwater temperature, T_{oh} [°C] is the outlet temperature in heating mode and COP is the coefficient of performance of the heat pump.

A mass flow rate equal to 23.5 L/s is found: this value is way lower than the available well flow, and consequently the GWHP system is feasible.

4.6 Central and decentralized storages

The size required for the central buffer storage for the new development district is evaluated by considering a value of 30 liters per kW of heating load [40]. A 20,000 L storage is then required to face the heat load of about 635 kW (considering only the heating demand).

The parameters for a 10,000 L storage tank of the company ENERPIPE are adopted, assuming that the technical information regarding a larger size will not differ much. An exception is the storage height, that is assumed doubled.

As stated in chapter 3, the decentralized storage solution is integrated in the project for several reasons: providing flexibility to the grid, covering peak loads and implementing sector coupling. Each single-family house has its own storage tank, while double- or multi-family buildings have more than one tank, in relation to the number of residential units. For example, DFHs are equipped with two storage tanks.

The design of the tanks is based on the practical experience of the company ENERPIPE, since specific standards are not available. The district heating grid charges the storage by means of a heat exchanger, that can be internal or external. If the heating load of the building is lower than 20 kW, an internal heat exchanger is adopted. An exception is made for buildings nr. 19 and 21 of the new development area: given the lower supply temperature of the grid, using an internal heat exchanger for these buildings turned out to be suboptimal.

The tanks chosen for the project are designed and manufactured by ENERPIPE and are available in volumes up to 1000 liters. The model HPDL is provided with an internal shell-and-tube heat exchanger, while the model ÜPDL is equipped with an external plate heat exchanger (Figure 4.6).

To allow implementation of sector coupling, each building is provided with a PV plant, that was dimensioned in the previous thesis by considering the available roof area [12]. The amount of PV power used for integrating the electricity and thermal sector is the surplus that is not consumed by the building for household electrical appliances. The data regarding the electricity demand for the buildings is taken from VDEW (*Verband der Ernährungswirtschaft*) standard hourly profiles [41], while the annual demand is based on 2021's Annual Electricity Review (*Jahresstromspiegel*) [42].

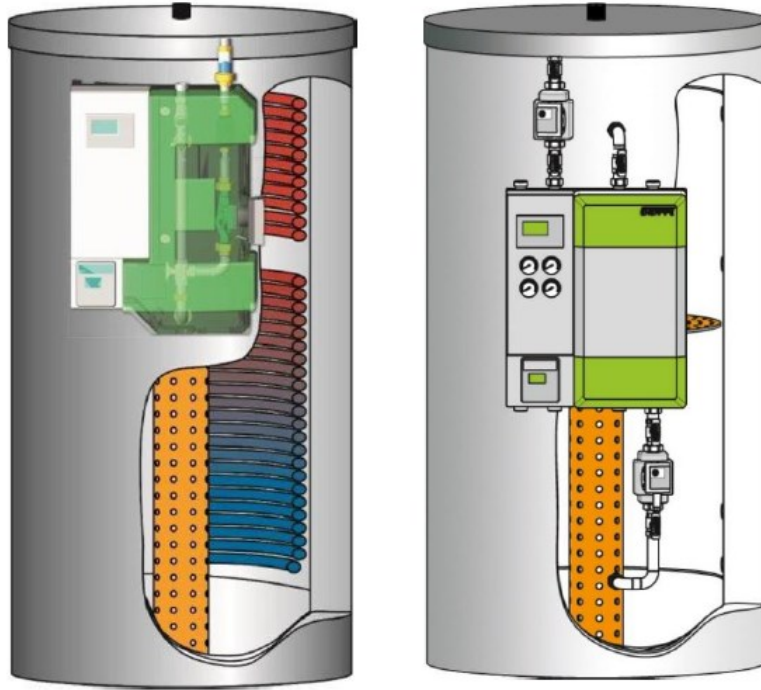


Figure 4.6 HPDL (left) and ÜPDL (right) storage tanks from the company ENERPIPE [43].

4.6.1 Electric elements

As stated before, electric elements are connected to the tanks belonging to single- and double-family houses. The elements are installed externally to the tank, according to the concept developed by ENERPIPE, so that better storage charging and temperature stratification is ensured. This concept is represented in Figure 4.7.

The design electric power is calculated by considering the DHW demand, since in summer the available surplus PV power is higher and in that period the heat demand is mostly related to DHW requirement of the buildings.

The calculation is made through an Excel sheet by taking into account a charging time of 6 hours:

$$P_{el,rod} = \frac{V_{storage} \cdot \rho_w \cdot c_{p,w}}{\Delta\tau_{charging}} [W], \quad (4.7)$$

where $V_{storage}$ [m³] is the storage volume, ρ_w [kg/m³] is water density, $c_{p,w}$ [J/kg·K] is the specific heat of water and $\Delta\tau_{charging}$ [s] is the charging time.

Power equal to 1 kW is obtained for all the electric heating elements that are considered.

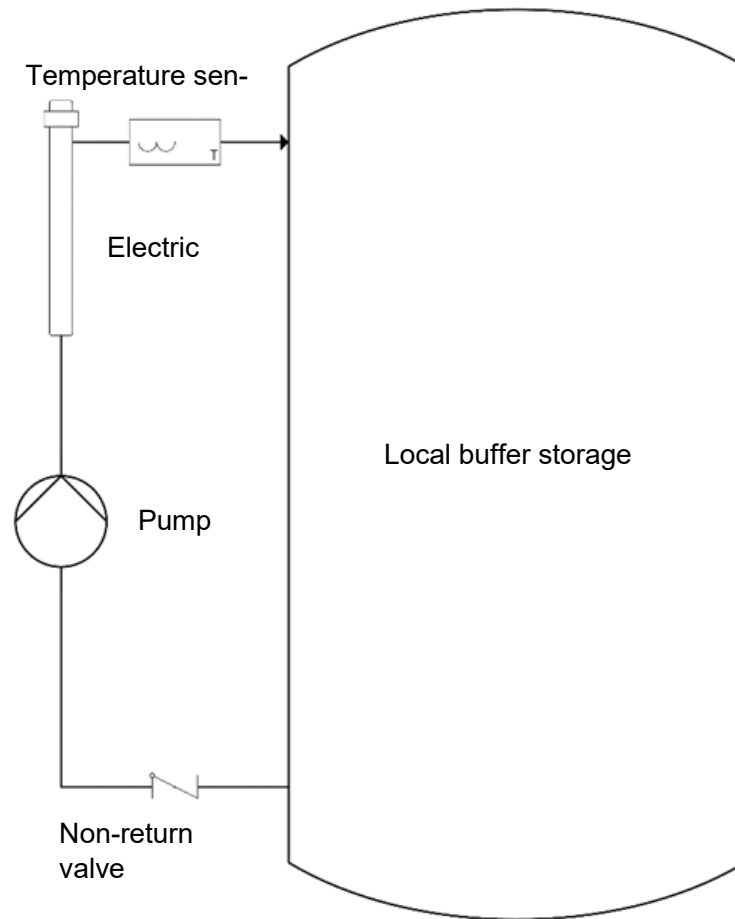


Figure 4.7 Storage concept, version with electric element [12].

4.6.2 Decentralized heat pumps

For the large MFHs located in the new development area, air-water heat pumps are connected to the storage instead of electric elements. There are four buildings of this type, but the number of connections and storage tanks is higher and corresponds to the number of residential units. This solution is adopted due to the higher demand of the MFHs and in order to keep low circulation losses and lengths of the pipes.

The design of the HPs is based on DHW demand since the main task of the coupling components is to keep the DHW supply at a suitable temperature level. The German standard DIN EN 15450 is followed [44]: according to it, the storage should be sized for the highest DHW demand: this allows to exploit PV availability fully and to avoid switching on and off the HPs too much.

The storage volume for the tanks connected to HPs is designed through equation (4.8), by considering the DHW load [44].

$$V_{storage} = 2 \cdot V_{DHW} + \frac{Q_{sto,losses}}{c_{p,w} \cdot (T_{sto,target} - T_{cold})} [L], \quad (4.8)$$

where V_{DHW} is the volume of the daily DHW demand, $Q_{sto,losses}$ [Wh/day] are the daily storage heat losses, $c_{p,w}$ [J/kg·K] is the specific heat of water, $T_{sto,target}$ is the target temperature [°C] for the storage and T_{cold} is the return temperature [°C] of the water in the DHW circuit.

For all the cases, a storage volume of 1,000 L is obtained: the model ÜPDL of ENERPIPE storage considered previously can be chosen.

The heating capacity of the decentralized HPs is then calculated as:

$$\dot{Q}_{h,HP} = \frac{Q_{storage}}{\Delta\tau_{HP}} [W], \quad (4.9)$$

where $Q_{storage}$ is the storage energy [Wh] and $\Delta\tau_{HP}$ is the storage charging time period, set to 3 hours.

The calculation results in 17 kW of required heating capacity for the HPs. Thus, the Ochsner air-water HP AIR 23 C12A [45] chosen in the previous thesis [12] is still suitable.

5 Simulation model

5.1 Software description

The software exploited for the thesis' work is the 2021b version of MATLAB [46], considering in particular the Simulink environment [47] for building the model and carrying on simulations. Simulink is a graphical environment that allows to simulate dynamical systems. These are built with blocks, connected through input and output signals representing the parameters that are involved in the calculations inside the different blocks. Simulink is able to call algorithms from MATLAB or to use it for pre- or post-processing purposes [48].

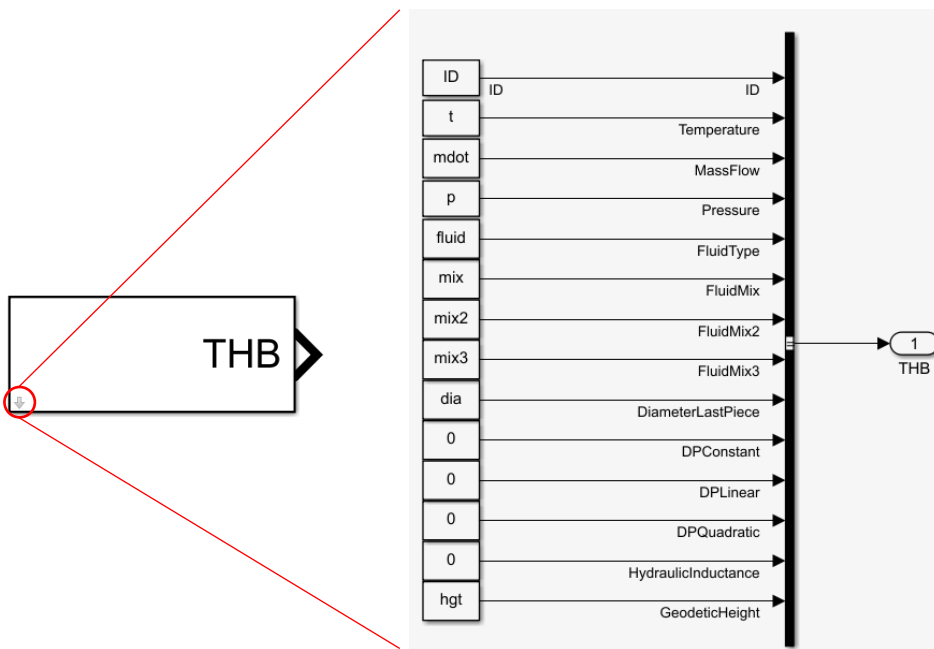


Figure 5.1 Basic THB block, with overview of the parameters that are carried by the signal [47].

The models built in this thesis are specifically created by using CARNOT (Conventional And Renewable eEnergy systems Optimization Toolbox), in version 7.3 [49]. This toolbox has been developed by the FH Aachen Solar Institute, and consists of an additional library for Simulink, that allows simpler modelling of thermal and electrical components used in HVAC systems, such as heat pumps, heat exchangers, pipes and valves. An important advantage of this library is the possibility to simulate hydraulics and heat transfer at the same time [50]. The key component of the library is a bus signal called THB (thermohydraulic bus), represented in its basic form in Figure

5.1. It represents different parameters related to the stream that is under consideration (for example the water flowing in the DHG), such as temperature and mass flow rate. Pressure evaluation is also possible, but was not considered neither in the previous work nor in this one, due to the very high computational effort and consequent simulation time [12]. Therefore, only a thermal simulation is carried out in this thesis.

5.2 Model development

The model is developed starting from the one created in the previous thesis [12], by making the required changes and additions: thus, comparison can be made in an easier way.

The main changes that had to be implemented, besides the new DHW demand calculation, are:

- Division of the DH grid into two different grids and consequent change of the pipes' parameters.
- Change of the supply temperature for the new development area and change of the minimum temperature for the sliding-mode operation of the existing buildings area.
- Introduction of the central heat pump in the new development area, together with a central buffer storage and related control strategy.
- The district heating grid is kept switched on even in summer, unlike what was considered in the sector coupling energy-route analyzed in the previous work.
- The number of connections between some houses and the DHG is increased proportionally to the number of actual residential units. Consequently, the number of required decentralized storage tanks is higher.
- New design for the electric elements and decentralized HPs.

These changes imply modifying some aspects of the decentralized storages, both regarding the geometry and the control strategies for the regulation of the charging.

Moreover, the models representing the storages are separated from the overall models of the two grids: a total of eight models (Table 5.1) is created, where the output data from the storage charging models are rearranged and used as input data for the overall grid models. This decision was made due to the high computational effort required by the high number of buildings connected to the grid. However, this approach has some limitations: the supply temperature considered in the storage models is assumed to be constant, neglecting the effects of heat losses along grid pipes, that lead to a temperature decrease in the heat transfer fluid.

Table 5.1 Developed Simulink models.

Model	Area	Involved buildings (nr. ¹)
Storage Heckenweg	Existing	1 to 27
Storage Heinrichsheimstraße HPDL	Existing	30 to 32, 34 to 41, 43, 44, 46, 47, 49, 50, 52 to 56
Storage Heinrichsheimstraße ÜPDL	Existing	28, 29, 33, 42, 45, 48, 51, 57
Storage HPDL	New development	58 to 72, 75
Storage ÜPDL	New development	73, 74, 76 to 78
Storage HP	New development	79 to 82
Overall grid	Existing	1 to 57
Overall grid with central HP	New development	58 to 82

5.2.1 Central heat pump

For the modelling of the central GWHP, the CARNOT heat pump block is used. However, a modified version of the block is taken into account [51]: the improvement with respect to the original block consists of considering the actual characteristic curves of the HP as inputs. These represent the heating and cooling capacity and the electric power consumption as functions of the source and supply temperatures, and can be found in the datasheets provided by HiRef [35].

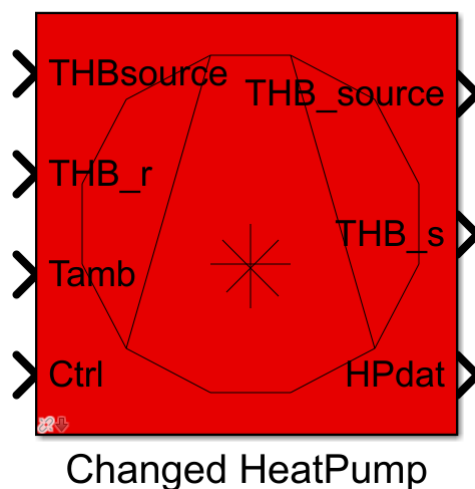


Figure 5.2 Modified heat pump block from the CARNOT library [49].

¹ In this case, the enumeration of buildings refers to the entire district.

As can be seen from Figure 5.2, the block requires as input the THB signal that represent the source (in this case, groundwater), the THB representing the DHG return, the temperature of the surroundings where the heat pump is working, and the control for switching on and off the component. The outputs of the block are the THB for the return side of the source, the THB for the supply of the DHG, the data regarding heating capacity, cooling capacity and electrical power consumed by the heat pump.

5.2.2 Central storage

The CARNOT library provides several blocks for representing storage tanks: the block “Storage_Type_1” is used for modelling the central storage for the new development area. As it is shown in Figure 5.3, the block requires four different inputs. These are the temperature of the surroundings where the storage is placed (T_{amb}), the THB signals related to charging and discharging, and eventually the electric power of a heating element, that in this case is not considered. The outputs of the block are data (temperature levels, changes in the storage energy content, thermal losses, etc.) regarding the storage (S_{dat}), the temperature values detected by the sensors ($T_{sensors}$) and the outlet THB signals for charging and discharging. Other parameters that have to be set by the user are the storage volume, the diameter of the tank, the heat transfer coefficients for the bottom and lower parts and thermal conductivity.

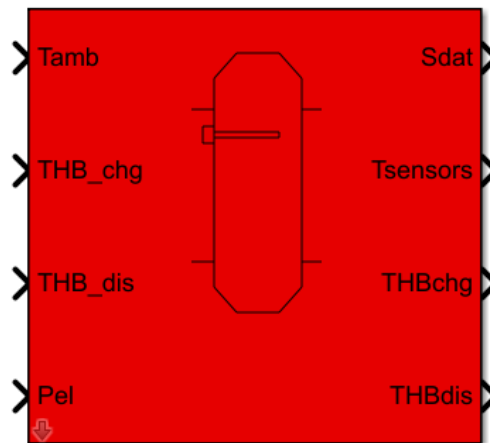


Figure 5.3 Type 1 Storage block from the CARNOT library [49].

As shown in Figure 5.4, the inlet for charging is located in the upper part of the storage tank. On the other hand, the DHG discharges the storage by withdrawing the required mass flow rate at a lower height, a bit above half of the tank height. The return side of the grid and of the HP are placed at the same height, almost in the lowest part of the storage tank.

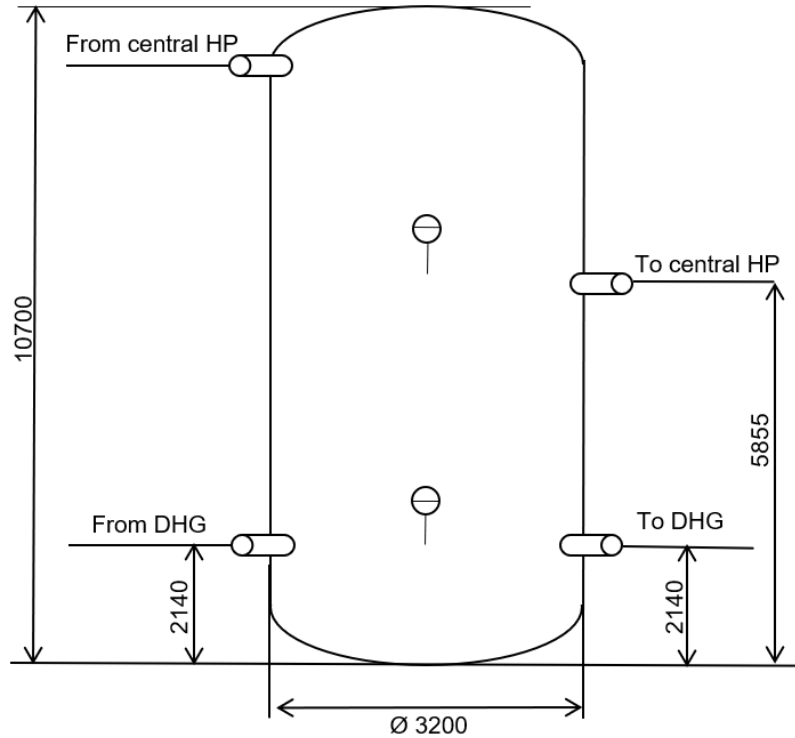


Figure 5.4 Input and output heights in the central storage (measures in mm).

Due to the large volume, the storage is expected to be placed outside and therefore the considered ambient temperature is the outdoor one.

5.2.3 Control strategy for central heat pump and storage tank

The control strategy for the GWHP and the storage was developed by considering the purpose of supplying the grid at the required temperature. The control is based on hysteresis, so that high frequency switching cycles are avoided. The HP is switched on and starts charging the storage when both the temperature correspondent to the outlet for the DHG drops 3 K below the upper threshold temperature, and the lower storage temperature drops 0.5 K the related threshold. The threshold temperatures are shown in Table 5.2. When the lower storage temperature is higher than the lower threshold, the charging is switched off.

Table 5.2 Threshold temperature for the control of the central storage tank's charging.

	Threshold temperature
Upper (DHG withdrawal)	48 °C
Lower	38 °C

Furthermore, the water mass flow that is required at the condenser of the HP, so that it provides the required supply temperature for the DHG (45°C), is regulated by taking into account the characteristic curve of the heating capacity, through a “Lookup Table” block. The block returns an output value depending on the input that is given, by looking up or interpolating a table of values that has to be defined with block parameters [47]. The mass flow is then calculated as in (5.1).

$$\dot{m}_{in,HP} = \frac{\dot{Q}_{heating}}{c_{p,w} \cdot \Delta T_{w,DHG}} \text{ [kg/s]}, \quad (5.1)$$

where $\dot{Q}_{heating}$ is the heating capacity of the heat pump for the design point [W], $c_{p,w}$ [J/kg·K] is the specific heat of water, $\Delta T_{w,DHG}$ is the difference between supply and return temperatures of the grid [K].

5.2.4 Decentralized storage tanks

The block “Storage_Type_3” is used and slightly modified to adapt to the two ENERPIPE tank models that are considered. The calculation is done by considering twelve equidistant temperature nodes along the height of the storage tank.

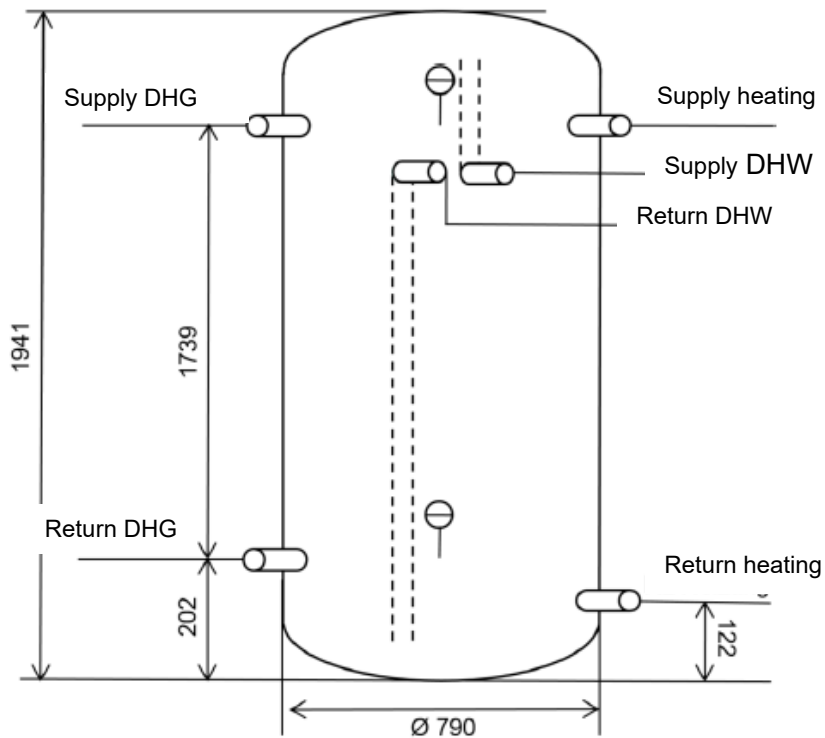


Figure 5.5 Input and output heights in the storage, heights are referred to the tanks for the existing buildings [12].

The heights of the inlets and outlets for the existing area are based on the actual design provided by ENERPIPE. As can be seen from Figure 5.5, the highest point is used for DHW withdrawal, so that the temperature is sufficiently high. Slightly below, but still in the upper part of the tank, the inlet of the district heating grid and the withdrawal for heating supply are located. Both the return point for the grid and the heating circuit are located in the bottom part of the storage. A reference ambient temperature of 13 °C is considered for these storages since it is assumed that they will be located in the basement of the buildings.

The block that represents the storage is shown both in Figure 5.6 and Figure 5.7, that represent the model for the decentralized storage tank with internal and external heat exchanger respectively. This type of storage block is more complex with respect to Type 1: it allows the connection to the DHW and heating circuits (bottom ports) and is equipped with two internal heat exchangers. However, only the upper heat exchanger is considered for the storage charging performed by the DHG. The bottom heat exchanger is removed, and its ports are used to connect the electric element or the air-water HP. The upper heat exchanger is also removed for the tanks that are equipped with an external heat exchanger, represented in Figure 5.7 by the “Heat Exchanger” block.

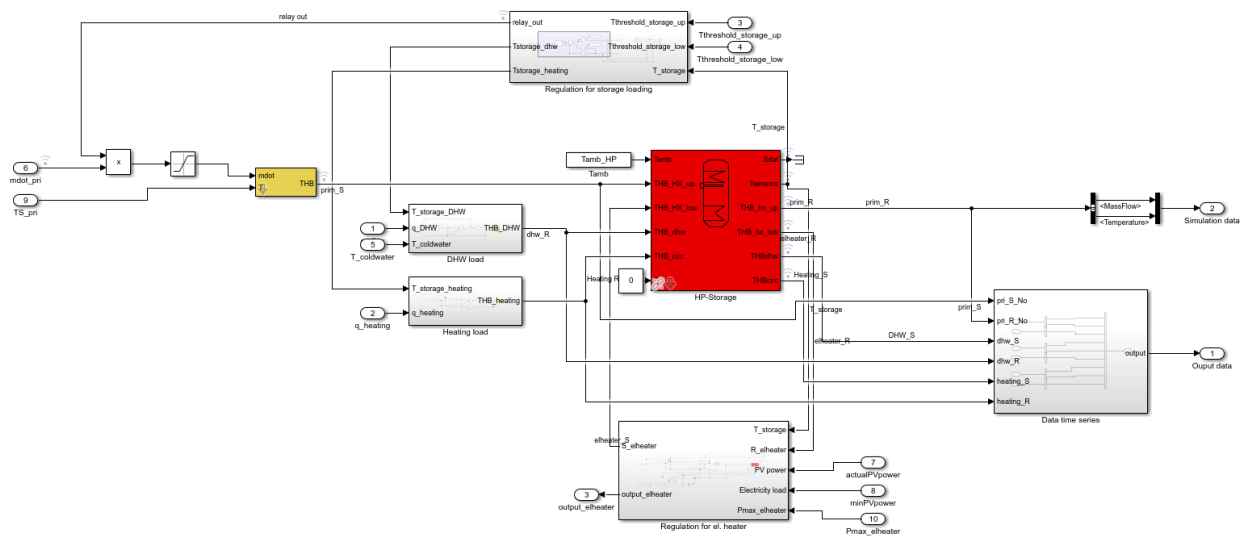


Figure 5.6 Model for the decentralized storage equipped with internal heat exchanger (HPDL) [49].

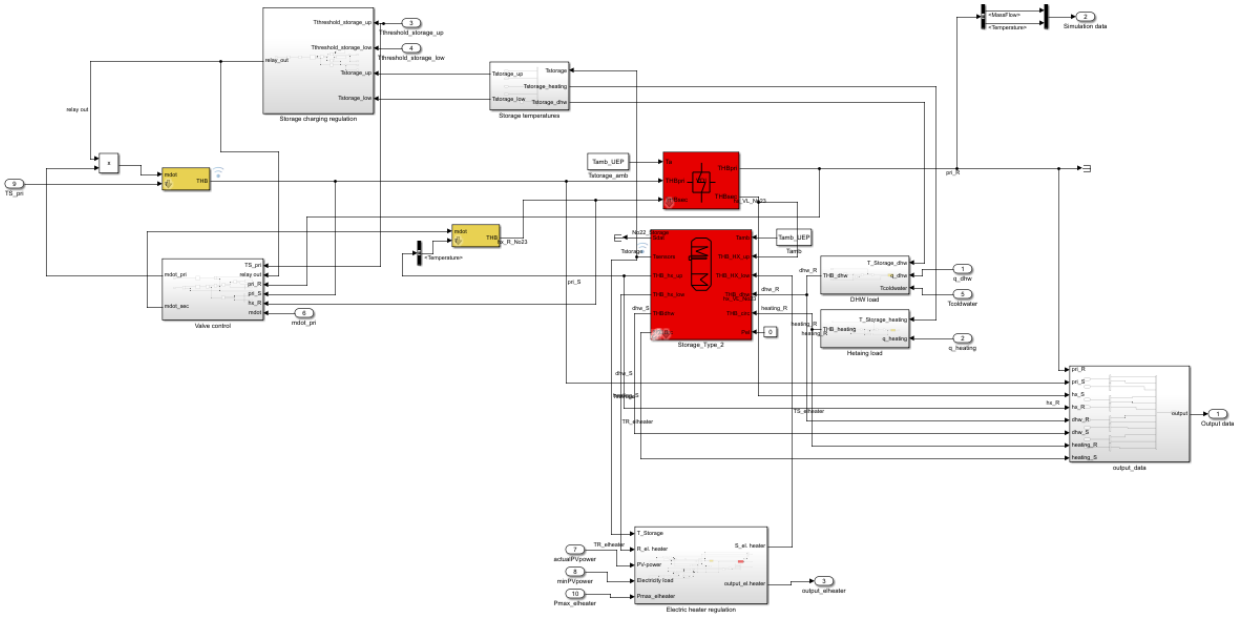


Figure 5.7 Model for the decentralized storage equipped with external heat exchanger (ÜPDL) [49].

Due to the lower grid supply temperature, the heights are modified in the new development district: the heating supply point is moved down, at 45% of the storage height, since the temperature level required by floor heating is lower. In this case the ambient temperature for the storage is set equal to 20 °C, because the new buildings will not be built with a basement, and consequently the storage tank is assumed to be placed inside the heated spaces.

The mass flow rate that is withdrawn from the storage tank is calculated as:

$$\dot{m}_{\text{withdrawn}} = \frac{\dot{Q}_{\text{load}}}{c_{p,w} \cdot \Delta T_{\text{storage}}} \text{ [kg/s]}, \quad (5.2)$$

where \dot{Q}_{load} is the required heating or DHW load [W], $c_{p,w}$ [J/kg·K] is the specific heat of water and $\Delta T_{\text{storage}}$ [K] is the temperature difference between inlet and outlet of the considered withdrawal.

The mass flow rate withdrawn for DHW purposes is related to the temperature difference between the point of withdrawal and the inlet cold water: this last temperature is represented in a simplified way along the year, through a sinus curve with minimum value of 6 °C in mid-February and maximum value of 14 °C in summer. As for the heating load, a fixed temperature difference equal to 11 K and a return temperature of 21 °C are assumed, this last value referring to room temperature. A maximum value for the mass flow rate is also set, equal to 1.5 kg/s.

The models for the DHW and heating circuits do not take into account the effects of the freshwater station and of the type of terminals respectively. These components are not modelled in Simulink, since the focus of the thesis is on the supply of the district as a whole, which is not affected by these components.

5.2.4.1 Control strategy

The storage control strategy created in the model mainly follows the one proposed by ENERPIPE: however, some modifications are necessary for the new development area, due to the lower temperature required for the heating supply. As for the case of the central storage tank, the control is based on hysteresis so that the number of loading cycles is kept low.

The district heating grid starts loading the storage when the temperature in the upper part of the tank falls 3 K and the lower storage temperature falls 4 K below the respective threshold temperatures. These temperatures are related to the minimum temperature requirements of the buildings and are shown in Table 5.3.

Table 5.3 Threshold temperature for the control of the decentralized storage tanks' charging.

Threshold temperature	Operation mode	Existing buildings	New buildings
Upper	Sliding-constant/constant	70-65 °C	45 °C
Lower	constant	55 °C	35 °C

For the existing buildings the upper threshold is set for the temperature required by radiators, while the lower threshold influences the grid return temperature; both temperatures are based on values considered by ENERPIPE. In the case of sliding-constant operation mode, the upper threshold temperature is changed depending on the allocation temperature. Consequently, the threshold is lowered in the warmer months due to the very low heating demand but making sure that sufficient high temperature for DHW supply is ensured. The storage charging goes on until the lower storage temperature reaches the threshold value.

5.2.4.2 Electric heating elements and decentralized heat pumps

The electric heating element is assumed to have 100% efficiency, implying that all the electrical energy is converted into heat. The element heats up the water withdrawn from the bottom part of the storage to the target temperature, set to 70 °C. This temperature, together with the required heat demand, influences the calculation for the charging mass flow rate.

The element starts charging the storage when PV surplus is available, that is when the PV feed-in exceeds the electricity demand. The excess that is not exploited by the element can be used for running partially the GWHP of the new development area: excess power is present when the surplus is higher than the set maximum power deliverable by the electric heating element.

The control strategy for the heating element is also based on hysteresis: if PV surplus is available, the element charges the storage up to the point when the lower storage temperature reaches the upper threshold of 60 °C. When the storage is completely charged, the element switches off and starts charging again only when the lower storage temperature drops to the lower threshold, that is set to 50 °C. This allows to maintain a not too fast on-off switching behavior. The threshold temperatures, showed in Table 5.4, are different for the new and the existing areas.

Table 5.4 Threshold temperatures considered in the control strategy for the heating element charging. Values that were considered for the existing buildings in the previous thesis are crossed out.

Circuit	Threshold temperature	Existing buildings	New buildings
PV surplus exploitation	Lower	50 °C	45 °C
	Upper	60 °C	50 °C
Emergency circuit	Lower	55 °C	60 °C
	Upper	68 °C	65 °C

An emergency circuit is included for the storage tanks in the new development area, due to the low grid supply temperature. The control strategy for this circuit is dependent on the upper storage temperature: when it drops below the lower threshold (Table 5.4), the element starts loading by exploiting either PV surplus or the electricity from the grid. The charging stops when the upper threshold is reached. This circuit was considered also in the previous thesis [12], with the values indicated in Table 5.4. However, in this work the circuit is not included in the storage models for

the existing area, due to the fact that the grid is not disconnected in summer and the grid supply temperature is sufficiently high for both heating and DHW provision.

As for the central HP, the modified CARNOT HP model is also used for representing the decentralized air-water heat pumps. A maximum supply temperature of 65 °C, deriving from the datasheet [45], is considered.

The control strategy for these components is very similar to the one considered for the heating element, but with set-point lower temperatures equal to 45 °C and 55 °C.

An additional difference from the electric element consists in a minimum power that the available PV surplus has to reach to start operation of the heat pumps. This value is set to 6 kW, assuming the heat pumps to be one stage.

5.2.5 Models for the grids

As stated in the previous chapters, two different district heating grids are considered: consequently, two different models for the existing and the new development area are created. For modelling the pipes, the block “Pipe Geometry” from the CARNOT library is used: it requires input parameters such as length, diameter and heat losses of the pipeline section that is considered. These parameters are taken from LOGSTOR technical data [33] and from the dimensioning performed in 4.2. The temperature of the ground surrounding the pipes, required in input, is represented with a sinusoidal curve as the inlet cold water in the DHW circuit, ranging between 6 °C and 14 °C. When the mass flow must be divided into different branches of the pipeline, the blocks “Flow Diverter” for supply lines and “Flow Mixer” for return lines are inserted in the grid. An example of house connection created by using these blocks is shown in Figure 5.8.

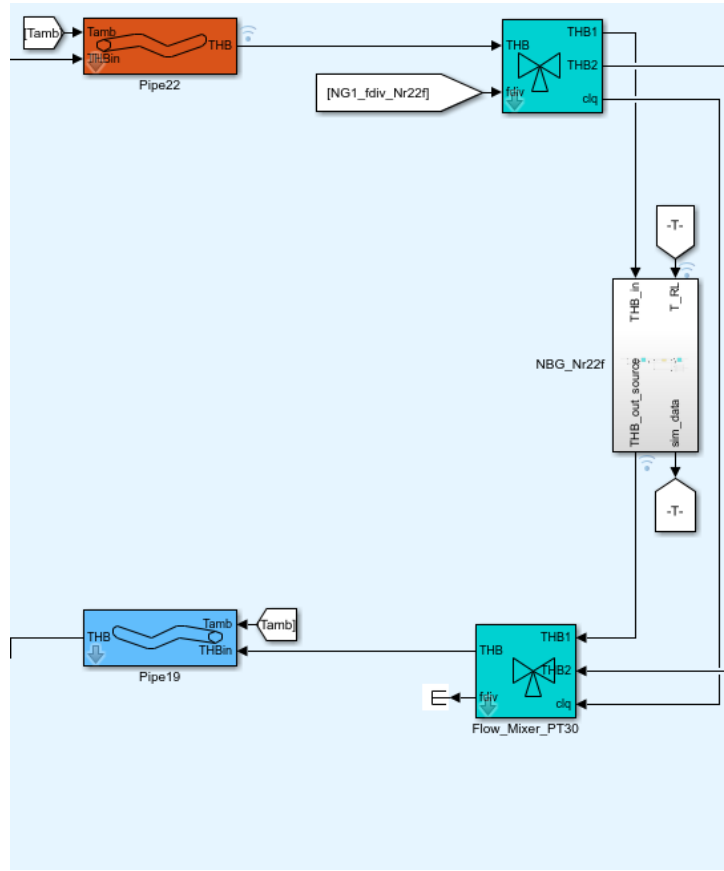


Figure 5.8 Representation of a house connection with supply pipe (red), return pipe (blue), flow diverter and flow mixer blocks (from the model created for the DHG for the new development area) [49].

An overview of the main features of the two grids is summarized in Table 5.5.

Table 5.5 Main features of the two DHGs.

DHG	Nr. house connections	Total pipe length (supply and return) [m]
Existing buildings area	57	2066
New development area	64	1418

The mass flow rates and return temperatures that are required as inputs for the simulations of the grids are taken from the storage simulations' results. Then, the return mass flow rate for the grid is calculated by taking into account the energy balance between the input heat demand \dot{Q}_{in} (resulting from the storage simulation) and the demand \dot{Q}_{DHG} in the grid simulation:

$$\dot{Q}_{in} = \dot{Q}_{DHG} \quad (5.3)$$

$$\dot{m}_{DHG} = \frac{\dot{m}_{in} \cdot \Delta T_{in}}{\Delta T_{DHG}} \text{ [kg/s]}, \quad (5.4)$$

where \dot{m}_{in} is the input mass flow rate (from storage simulation) [kg/s], ΔT_{in} is the ideal temperature difference between supply and return in the tank [K] and ΔT_{DHG} is the same temperature difference [K], but in the grid simulation.

6 Simulation results

The dynamic thermal simulations were carried out by using the variable step automatic solver in Simulink, considering a time frame of one year. The chapter presents some relevant results such as the required primary energy, the heat losses in the grid and in the storages and the GHG emissions. When applicable, comparisons with the reference scenario without sector coupling and with the first scenario considered in the Hybrid_BOT project are analyzed.

6.1 Photovoltaic surplus and heat demand

Figure 6.1 shows the heating and DHW monthly demands together with the PV surplus resulting from the difference between the PV production and the electricity demand of the buildings.

As would be expected, the heating demand is very high in the coldest months (January and December), while it is almost absent in summer, especially in August. On the other hand, DHW demand is almost constant throughout the year. It can be seen that more PV surplus (as well as PV production) is available during the summer months, due to higher solar irradiation and light hours.

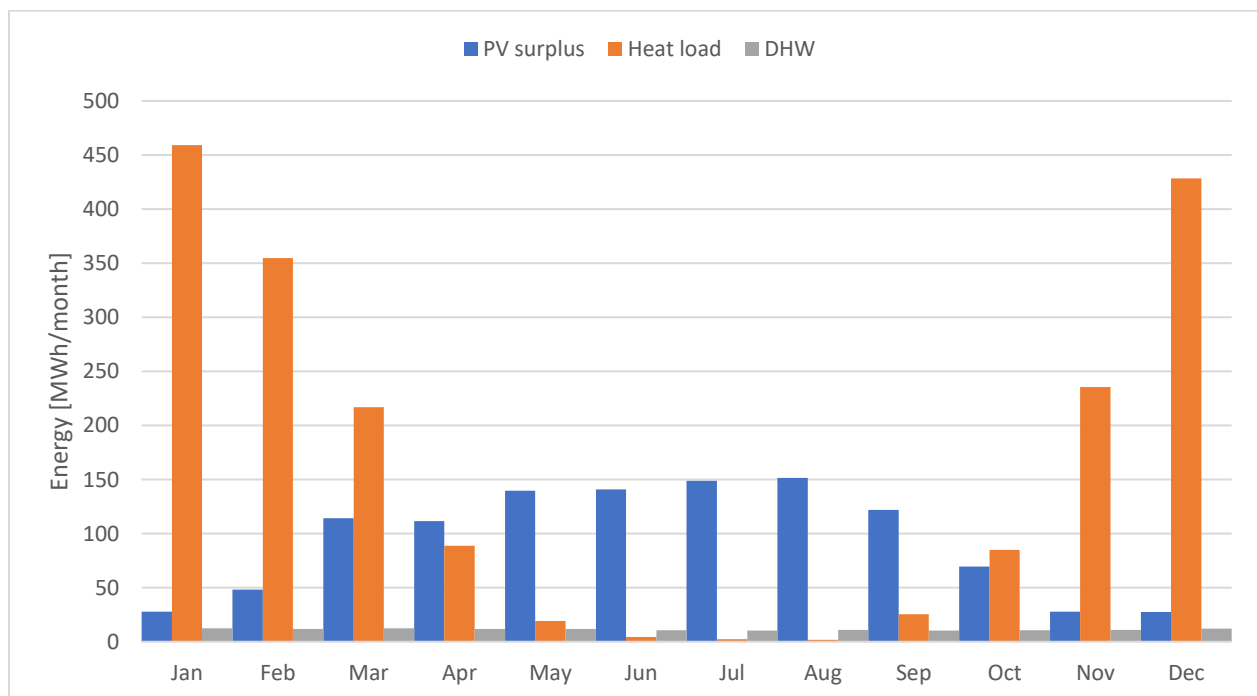


Figure 6.1 Monthly PV surplus, heating demand and DHW demand for the Heckenweg district.

6.2 Usage of the sector coupling technologies

As expected, the usage of the sector coupling technologies is higher during summer, due to the increased availability of PV power. This can be clearly seen from Figure 6.2, that shows that the grid is responsible for only 8-20% of the heat supply during the months of June, July and August. The operation of the sector coupling technologies is also higher than 50% in the mild months of May and September.

Another interesting result is that a still relevant share of heat supply is given by sector coupling during winter. Since the decentralized buffer storages are utilized to provide both heating and DHW demand, the lower supply temperature of the DHG serving the new development area implies that the coupling technologies operate also when PV power is not available, to ensure that the minimum requirement for the DHW temperature is maintained.

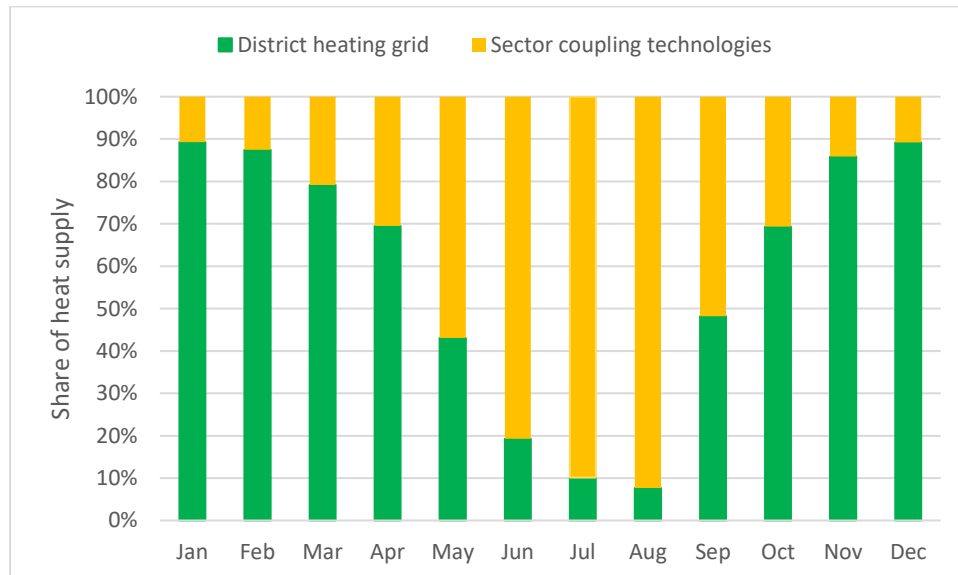


Figure 6.2 Shares of heat supply for the second energy route.

This explains why the share of electricity coming from the grid is higher in this energy route compared to the first one, as it is shown in Figure 6.3. However, since the DHGs of the second scenario are also operated in summer, the total exploitation of sector coupling technologies is lower with respect to the first scenario.

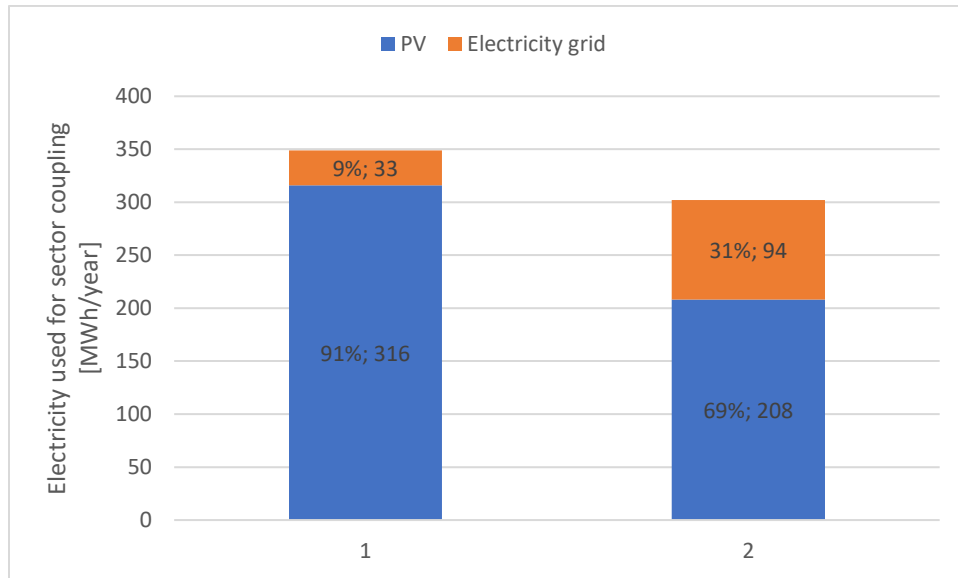


Figure 6.3 Comparison of the shares of electricity for sector coupling in the two energy routes.

6.3 Energy supplied by the district heating grids and heat losses

The energy supplied to the Heckenweg district by the two DHGs is shown in Figure 6.4, where the duration curve is compared with the curves related to the other two scenarios. It is clearly visible that in all scenarios the grids are operating at partial load most of the year: in all cases, the supplied power is higher than 700 kW only for about 800 hours a year, during winter. In this season, the different curves have almost the same behavior. During the rest of the year, the heat power supplied by the DHGs in the energy routes is lower compared to the reference scenario: this is mostly due to the implementation of sector coupling, which can partially or totally replace the grid, especially during the summer months. The two curves for the energy routes with sector coupling behave in a similar way during summer, but it is visible that the grids of the second scenario are not shut down in summer. During the rest of the year, however, these DHGs supply a lower amount of heating power compared to the first scenario. This is attributable to the fact that the coupling technologies are exploited during the whole year, due to the lower temperature of the DHG for the new development area (see 0). The lower DHW load is also a reason for this, even if in any case the heating load (that is the same for all scenarios) is dominant.

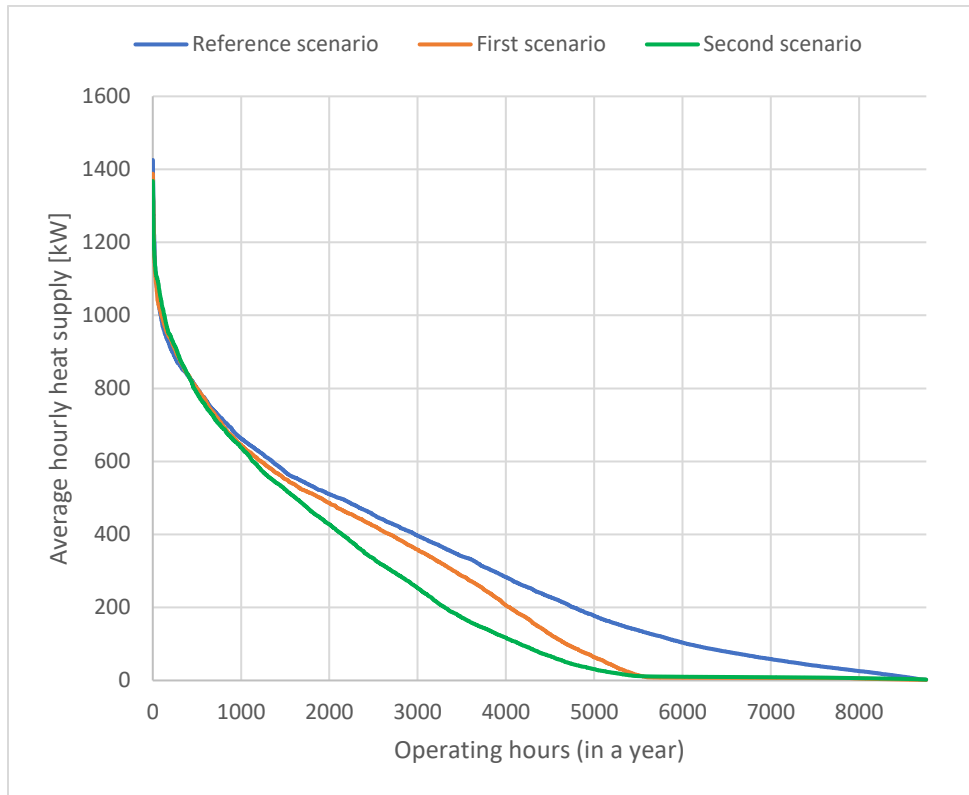


Figure 6.4 Duration curves of the different scenarios.

For the same reasons, the final energy supplied to the buildings by the DHGs in the second scenario is 30% and 20% lower than the reference and the first scenario respectively (Figure 6.6).

Regarding heat losses, the comparison between the two DHGs operated in the second energy route is shown in Figure 6.5. The heat losses for each DHG are exclusively calculated by considering the difference between the energy provided by the grid and the amount of energy withdrawn in correspondence of the house stations, considering both heating and DHW requirements. Considering the percentage values, Figure 6.5 shows that the lower supply temperature of the DHG of the new development area implies lower heat losses, thanks to the lower temperature difference between the water flowing in the pipes and the surrounding ground, compared to the DHG serving the existing buildings area.

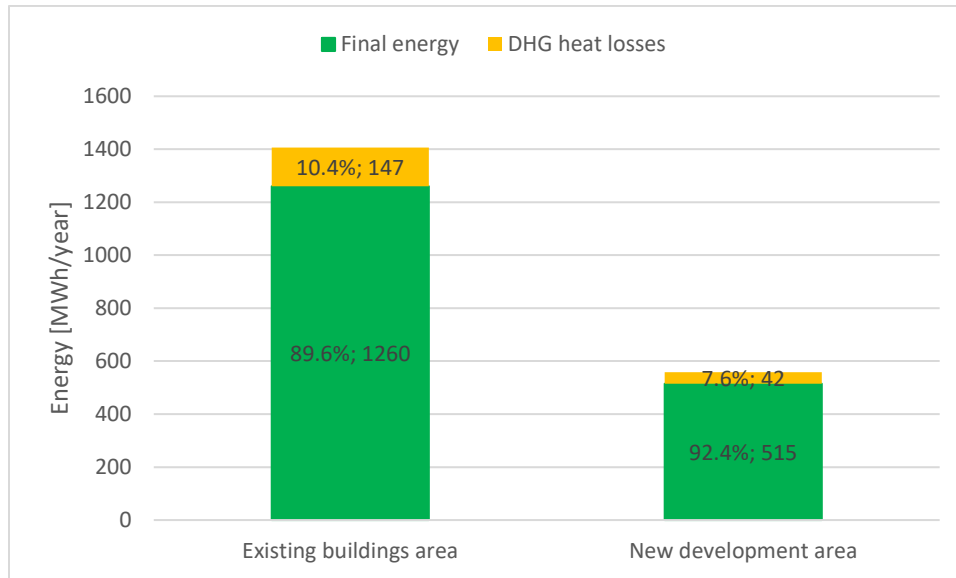


Figure 6.5 Comparison between the two DHGs operated in the second energy route, regarding final energy supplied and heat losses of the grid.

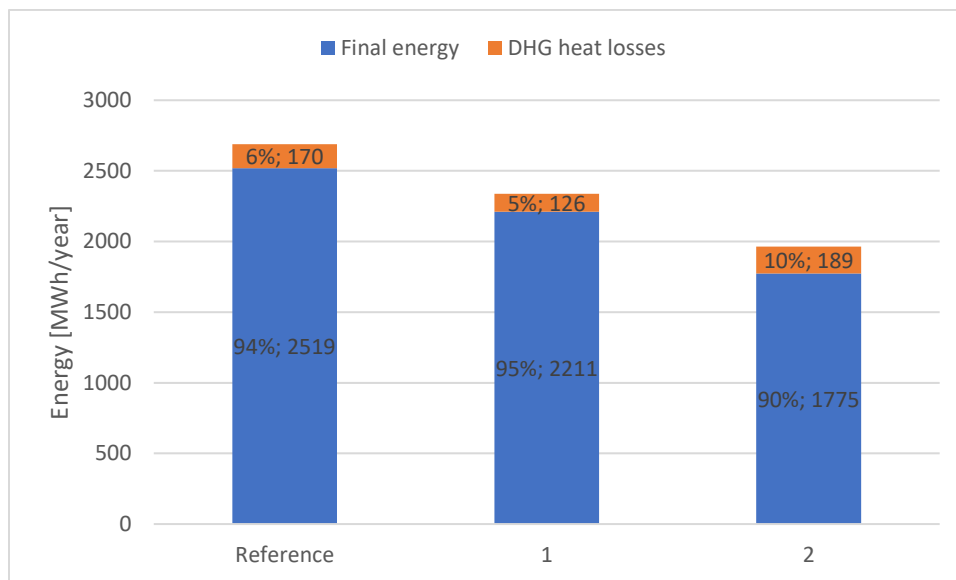


Figure 6.6 Final energy supplied and heat losses of the grid, comparison among the different scenarios.

On the other hand, Figure 6.6 shows that despite the employment of a LTDH for the new development area, the heat losses for the whole district are higher compared to the other two scenarios. This is explained by the lower considered DHW demand, that results in less DHW withdrawal and consequently in lower heat density. Moreover, Figure 6.7 shows that for the second energy route the losses are very high in summer, especially during June, July and August. This is due to the fact that the grid is operated even when the mass flow rates and consequently the difference

between supply and return temperatures are very small, determining heat losses in the pipes. The mass flow rate circulating in the DHW circuit is very small in summer not only due to the exclusive presence of the DHW load, but also because most of this requirement is fulfilled by the coupling technologies, as can be seen from Figure 6.2. A possible solution to this issue could be to switch off the grid in summer, so that the DHW requirement is completely met by the sector coupling technologies.

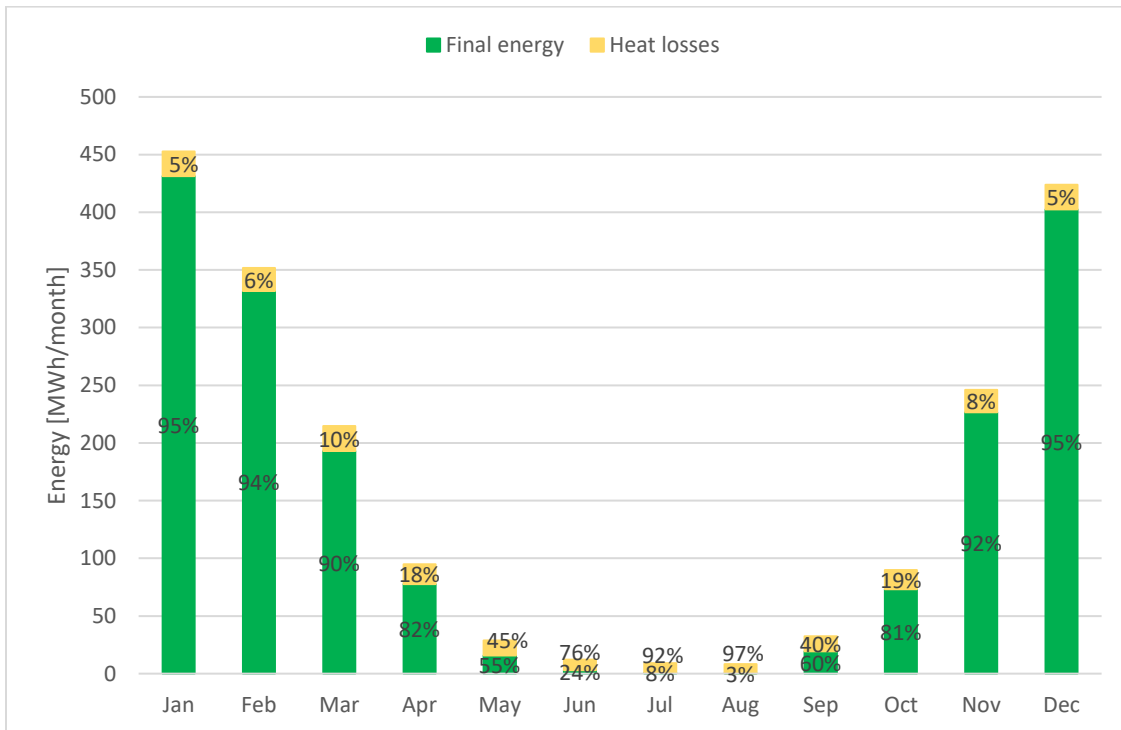


Figure 6.7 Monthly values for the final energy delivered by the DHG and correspondent heat losses for the second energy route.

6.4 Pump energy

The electrical energy required by the grid pumps along the year is obtained from the related curve obtained through the online tool Wilo-Select [34]. The mass flow values that are considered derive from the simulation results of the two grids. The values of energy for the two pumps are summed, so that the pump requirement for the overall district can be calculated and compared with the other scenarios.

In general, the energy required by the grid pump in one year should account for 0.5-1% of the heat energy supplied by the grid [28]. As can be seen from Figure 6.8, the obtained result for

the analyzed scenario is in line with this empiric value: the electricity required for the two pumps is equal to about 10 MWh/year, accounting for 1% of the heat supplied by the DHGs.

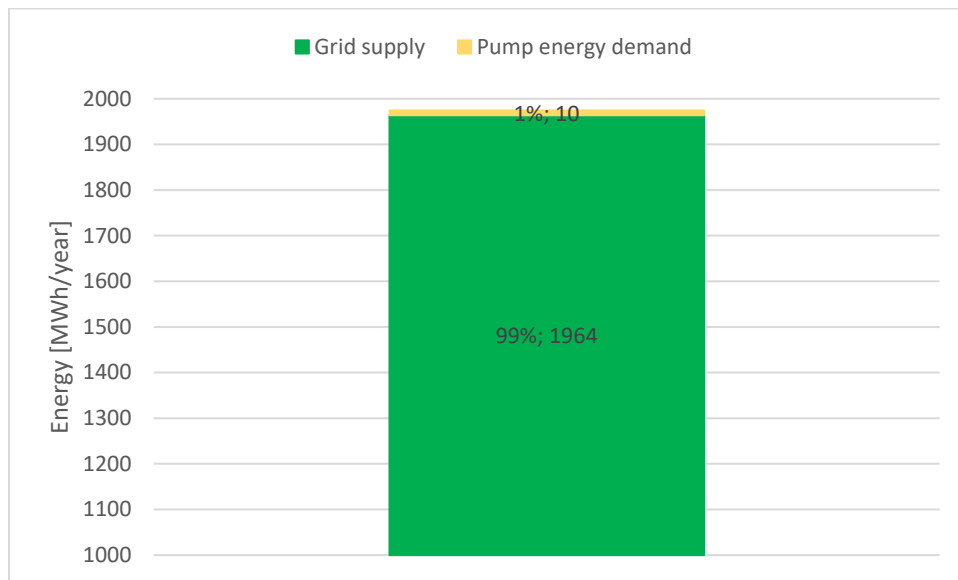


Figure 6.8 Shares of energy supplied by the two DHGs and of the energy required by the grids' pumps for the second energy route.

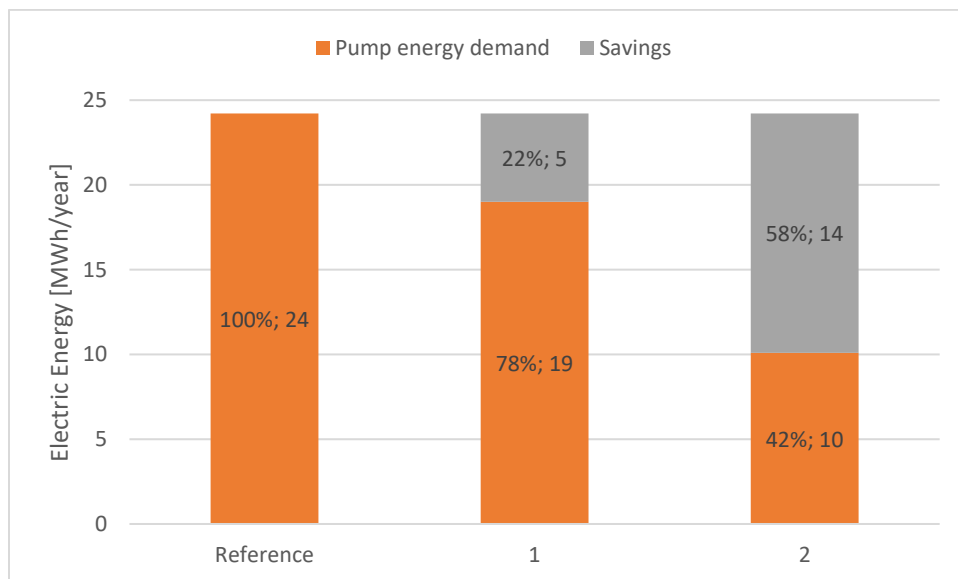


Figure 6.9 Pump energy demands and the savings of the sector coupling energy-routes with respect to the reference scenario.

Data in Figure 6.9 show that the pumping power required for the two grids of the second scenario results in relevant savings with respect to both the reference (58%) and first (47%) scenarios. This can be explained by the fact that two separated grids are considered: even if two pumps are then

required, the mass flow that they must be able to process is lower. Moreover, the energy supplied by the grids is lower in the second energy route, that consequently requires less pumping power to be operated.

6.5 Primary energy

Primary energy is defined as the total amount of source energy, available in its natural form, that is required for supplying the final energy to the considered system [52]. In general, primary energy must be converted at least once before being available in the final form; the impact of transport has also to be taken into account. Thus, primary energy results from the sum of the final energy and the conversion losses.

Primary energy can be evaluated through (6.1) [52]:

$$Q_{primary} = Q_{final} \cdot PEF, \quad (6.1)$$

where $Q_{primary}$ is the primary energy consumed, Q_{final} is the final energy supplied and PEF is the primary energy factor.

The primary energy factor is a fundamental parameter that allows to compare the contribution of different energy carriers. However, it should be kept in mind that this is not the only method to calculate primary energy, and the usage of different methods can lead to different results.

The PEFs considered here are listed in Table 6.1. The values for PV and electricity network are taken from the German standard DIN V 18599-1 [53], while the value for waste heat is given by SWND [54], referring to the DHG already present in the town.

Table 6.1 PEF values for the different considered sources [52], [53].

Source	PEF
Waste heat	0.24
PV	0
Electricity network	1.8

Part of the electricity required by the central HP is supplied by the residual PV that is not used by the coupling technologies, while the remaining part is withdrawn from the electricity grid.

The evaluated primary energy values are shown in Figure 6.10 and compared with the reference scenario and the first energy route. For better clarification, the energy withdrawn from the electricity grid for feeding the sector coupling technologies is distinguished from the one that is used for supplying the central GWHP and from the one that is required for the pumps.

It is evident that the second energy route is characterized by a significantly higher consumption of primary energy, about four times the consumed amount of the other two scenarios. The main reason for this result is the high share of electric power required by the big GWHP that rooftop PV plants are not able to provide, and that thus must be fed by the electricity grid, which is characterized by the highest value of PEF among the sources that are considered here.

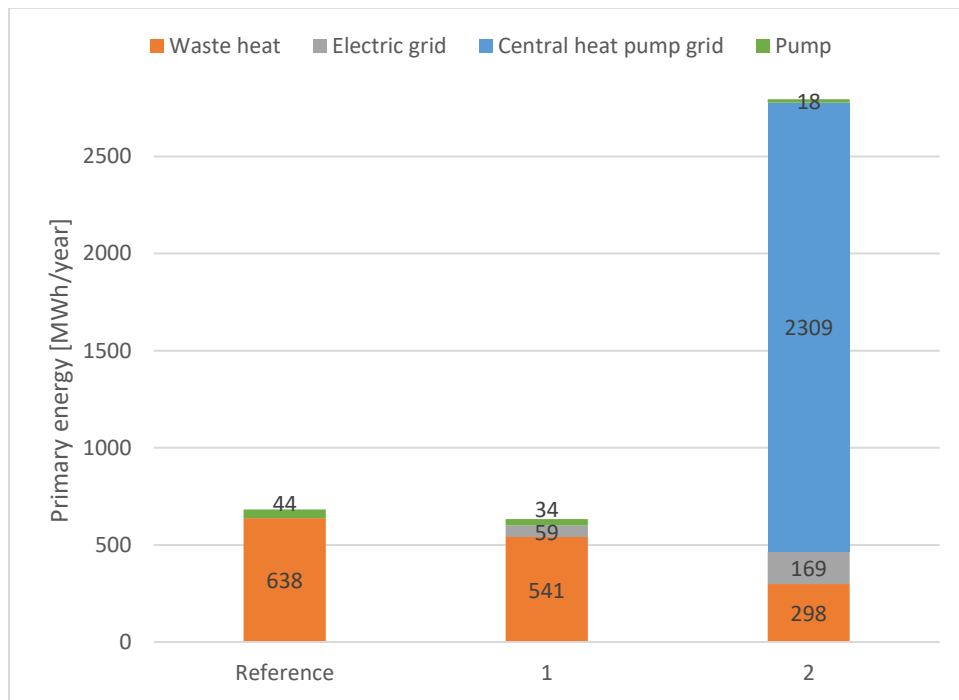


Figure 6.10 Primary energy for the different heat supply scenarios.

6.6 Greenhouse gas emissions

The CO₂ equivalents that are considered for the calculation of GHG emissions are shown in Table 6.2. They refer to the values given in [54], where a specific analysis about the grid already present in Neuburg an der Donau is presented.

Table 6.2 CO₂ equivalent values for the different sources [53].

Source	CO ₂ equivalent [g/kWh]
Waste heat	508
PV	0
Electricity network	550

The GHG emissions are then calculated by multiplying the CO₂ equivalent for each source by the respective primary energy.

The results of this evaluation are shown in Figure 6.11 and are compared to the reference and first scenarios. Since the calculation is strongly dependent on the primary energy consumption, the GHG emissions related to the second scenario are more than four times higher than the emissions of the other scenarios.

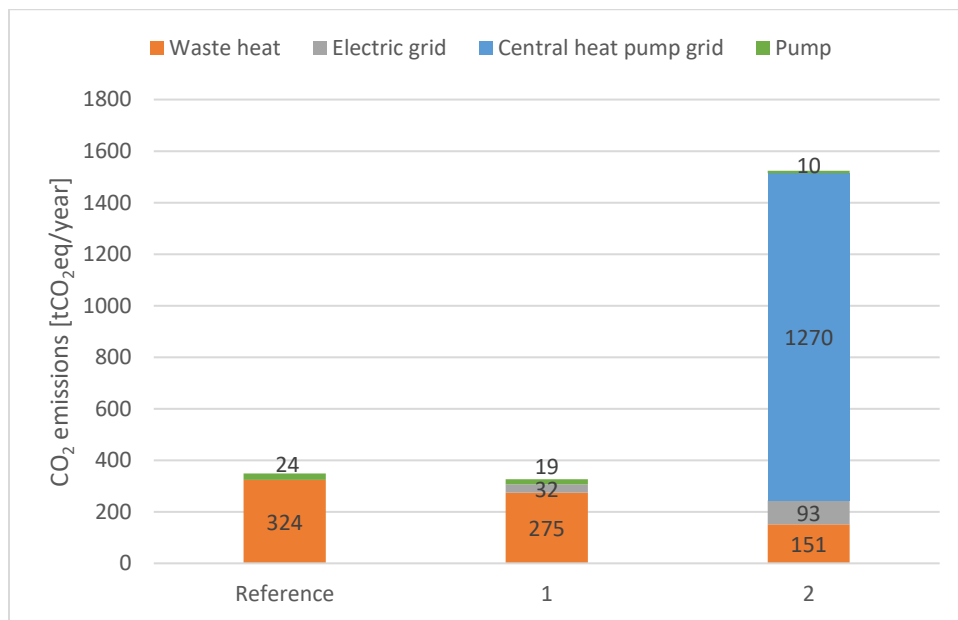


Figure 6.11 GHG emissions for every scenario.

However, it can be easily noticed that if the electricity required by the GWHP was supplied by PV power, the second scenario would imply a significant saving both regarding primary energy and GHG emissions. This could be achieved by installing a ground PV plant, that could be placed in the unoccupied fields located next to the Heckenweg district, as highlighted in Figure 6.12.



Figure 6.12 The available area that could be exploited for the installation of a ground PV plant [55] is highlighted in red.

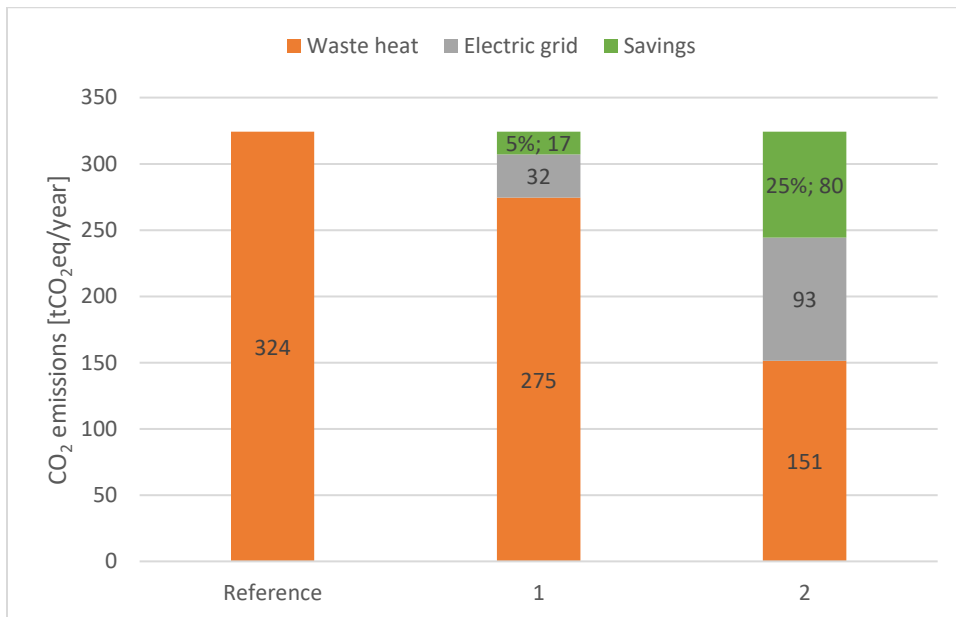


Figure 6.13 GHG emissions in case the HP for the second energy route was completely supplied by PV power, and savings with respect to the reference case.

Ideally, providing all the electricity required by the GWHP through PV would imply a decrease in GHG emissions of 25% with respect to the reference case and 19% with respect to the first energy route (Figure 6.13). However, it is necessary to keep in mind that in any case PV is an intermittent source: this means that even by exploiting a plant mounted on the ground, the electricity provided by it could probably not be sufficient to cover winter operation without an electricity storage system and without partially relying on the electricity grid.

7 Conclusion and outlook

A heat supply concept (second energy route) including hybrid district heating networks has been investigated in this work. The Heckenweg district in the German town of Neuburg an der Donau has been considered, and a comparison with a reference scenario and with another scenario exploiting sector coupling (first energy route) has been made. The district includes different types of houses, such as single- and multi-family houses, and both older existing buildings and new buildings that have not been built yet.

As described in 3, while the reference scenario only implies supply from the DHG, the two energy routes include hybrid DHGs exploiting sector coupling technologies, which are integrated in decentralized thermal storage systems. The electricity required for these technologies is provided through supply-oriented exploitation of rooftop PV plants, installed in every building. In the reference and first scenario the buildings are supplied by an existing DHG exploiting waste heat, with a supply temperature of 80 °C. The second proposed scenario, that is the focus of this thesis, is instead based on two different DHGs. The existing buildings area is still supplied by the already present DHG, while the new development area is served by a LTDH system including a central GWHP with storage, with a supply temperature equal to 45 °C which better matches the requirement for the floor heating systems.

The DHGs and the components included in the second energy route have been sized and modelled, and control strategies for the different thermal energy storages have been implemented. Yearly thermal simulations have been carried out in the software Simulink [47], and relevant results have been analyzed.

The supply concept is able to further allow integration between the heat and electricity sector, thanks to the presence of the central HP for the supply of the new development area. The LTDH system is also characterized by less heat losses compared to the DHG supplying the existing buildings area. However, there are some critical aspects that have emerged from the analysis of the results, and that are expected to be addressed in the next months in the context of the Hybrid-BOT_FW project (see 1.2).

The lower temperature supply for the new development area implies that the DHW minimum temperature requirement is actually not met, and consequently requires significant operation of the electric elements and decentralized HPs also during winter.

The network heat losses result to be higher compared to the other two scenarios, especially during summer operation: in fact, the DHW load considered for the second energy route is smaller, and

consequently the heat density is lower. Moreover, a significant amount of the DHW requirement is actually supplied by exploiting the storage coupling technologies, not only during the warmest months. These losses could be partially reduced by switching off the grid in summer, as was chosen for the first energy route.

Another consideration that can be made in this regard, is whether the decentralized buffer storage concept should be questioned for the new development area. In fact, in this case two different temperature levels are required for heating and domestic hot water, and inevitably the storage coupling technologies are also indirectly feeding the heating requirement, even if this is not needed. Moreover, the DHG supply temperature is in any case not able to provide the required minimum temperature for DHW. Consequently, a more efficient solution could be to supply the heating terminal circuits directly through the DHG and consider only decentralized DHW storage tanks for increasing the domestic water temperature to the level required to avoid the risks for hygiene.

Another important point regards primary energy consumption and GHG emissions, that are strictly correlated. The utilization of a central HP for the new development area implies the increase of the electricity requirement, that despite the initial concept formulated in the HybridBOT context, cannot be completely provided by the residual PV surplus of the rooftop plants. Thus, most of the electricity has to be withdrawn from the electricity grid, determining an increase in the primary energy consumption, and consequently in the GHG emissions, of about four times compared to the other scenarios. However, it is important to notice that this result is highly dependent on how the calculation of the primary energy is performed. First, this does not take into account the very high efficiency (COP) of HPs, especially the ones exploiting sources at almost constant temperature such as groundwater. Moreover, in this case the results are particularly discouraging because the comparison with scenario with a large share of waste heat is involved: normally large amounts of waste heat are not available for DHG operation. In addition, according to the German regulation for the calculation of the PEFs, waste heat recovered from the flue gases of CHP plants is not affected by the losses between primary and final energy, that are mostly allocated to electricity [56].

An aspect worth noting is that if ideally all the electricity for the HP was provided by PV, the values of primary energy and GHG emissions would be lower both with respect to the reference scenario and to the first energy route. This could partially be realized by considering a ground PV plant to be installed on the available area next to the district. However, this also draws attention to an important point that should not be neglected: the decarbonization of the heating sector cannot be

disconnected from the decarbonization of the other energy sectors, and especially from the electricity sector.

Even though some possible improvements have been identified, the energy route here analyzed has the potential to become an exemplary case for other districts, especially since large amounts of waste heat energy are not usually available. Moreover, the exploitation of the HP technology is characterized by high efficiency and gives the possibility to further integrate the electricity sector into the heating sector.

Literature

- [1] “Greenhouse Gas Emissions from Energy Data Explorer – Data Tools,” *IEA*. <https://www.iea.org/data-and-statistics/data-tools/greenhouse-gas-emissions-from-energy-data-explorer> (accessed May 05, 2023).
- [2] “The Paris Agreement | UNFCCC.” <https://unfccc.int/process-and-meetings/the-paris-agreement/the-paris-agreement> (accessed Nov. 22, 2022).
- [3] “Climate Action in Figures – Facts, Trends and Incentives for German Climate Policy,” p. 68, 2021.
- [4] “Germany - Countries & Regions,” *IEA*. <https://www.iea.org/countries/germany> (accessed Jan. 03, 2023).
- [5] “Anwendungsbilanzen zur Energiebilanz Deutschland - Endenergieverbrauch nach Energieträgern und Anwendungszwecken.” 2021.
- [6] A. R. Mazhar, S. Liu, and A. Shukla, “A state of art review on the district heating systems,” *Renew. Sustain. Energy Rev.*, vol. 96, pp. 420–439, Nov. 2018, doi: 10.1016/j.rser.2018.08.005.
- [7] K. Schmitz, “AGFW | Der Energieeffizienzverband für Wärme, Kälte und KWK e. V.,” p. 36, 2019.
- [8] K. Schmitz, “AGFW | Der Energieeffizienzverband für Wärme, Kälte und KWK e. V.,” p. 36, 2018.
- [9] H. Averfalk *et al.*, “Low-Temperature District Heating Implementation Guidebook. IEA DHC Report,” p. 206, 2021.
- [10] G. Goetzl, K. Zosseder, A. Vranjes, C. Schiffelechner, J. Chicco, and R. M. Singh, “Geothermal Heating and Cooling Networks for Green and Livable Urban Transformations – Part I,” 2021.
- [11] Fraunhofer IEE, AGFW, BBH, ENERPIPE, IKEM, and SWND, “Verbundvorhaben: EnEff:Wärme: HybridBOT FW. Transformation und Betriebsoptimierung von Wärmenetzen für die Entwicklung hybrider Netzstrukturen zur netzdienlichen Quartiersversorgung. General project description.” 2021.
- [12] L. Wett, “Simulationsgestützte Analyse und Bewertung ausgewählter Versorgungsvarianten eines multivalenten Wärmenetzes unter Berücksichtigung der Sektorenkopplung in Neuburg an der Donau,” Universität Kassel, 2022.
- [13] H. Lund *et al.*, “4th Generation District Heating (4GDH),” *Energy*, vol. 68, pp. 1–11, Apr. 2014, doi: 10.1016/j.energy.2014.02.089.
- [14] D. Schmidt and A. Kallert, “Future Low Temperature District Heating Design Guidebook. IEA DHC Report,” 2017.
- [15] A. M. Jodeiri, M. J. Goldsworthy, S. Buffa, and M. Cozzini, “Role of sustainable heat sources in transition towards fourth generation district heating – A review,” *Renew. Sustain. Energy Rev.*, vol. 158, p. 112156, Apr. 2022, doi: 10.1016/j.rser.2022.112156.

- [16] S. Buffa, M. Cozzini, M. D'Antoni, M. Baratieri, and R. Fedrizzi, "5th generation district heating and cooling systems: A review of existing cases in Europe," *Renew. Sustain. Energy Rev.*, vol. 104, pp. 504–522, Apr. 2019, doi: 10.1016/j.rser.2018.12.059.
- [17] P. Sorknæs, "Hybrid energy networks and electrification of district heating under different energy system conditions," *Energy Rep.*, vol. 7, pp. 222–236, Oct. 2021, doi: 10.1016/j.egy.2021.08.152.
- [18] C. Bernath, G. Deac, and F. Sensfuß, "Influence of heat pumps on renewable electricity integration: Germany in a European context," *Energy Strategy Rev.*, vol. 26, p. 100389, Nov. 2019, doi: 10.1016/j.esr.2019.100389.
- [19] A. Bloess, W.-P. Schill, and A. Zerrahn, "Power-to-heat for renewable energy integration: A review of technologies, modeling approaches, and flexibility potentials," *Appl. Energy*, vol. 212, pp. 1611–1626, Feb. 2018, doi: 10.1016/j.apenergy.2017.12.073.
- [20] O. Gudmundsson, J. E. Thorsen, and M. Brand, "The role of district heating in coupling of the future renewable energy sectors," *Energy Procedia*, vol. 149, pp. 445–454, Sep. 2018, doi: 10.1016/j.egypro.2018.08.209.
- [21] M. Werner, S. Muschik, M. Ehrenwirth, C. Trinkl, and T. Schrag, "Sector Coupling Potential of a District Heating Network by Consideration of Residual Load and CO2 Emissions," *Energies*, vol. 15, no. 17, p. 6281, Aug. 2022, doi: 10.3390/en15176281.
- [22] H. Averfalk, P. Ingvarsson, U. Persson, M. Gong, and S. Werner, "Large heat pumps in Swedish district heating systems," *Renew. Sustain. Energy Rev.*, vol. 79, pp. 1275–1284, Nov. 2017, doi: 10.1016/j.rser.2017.05.135.
- [23] R.-R. Schmidt and B. Leitner, "A collection of SWOT factors (strength, weaknesses, opportunities and threats) for hybrid energy networks," *Energy Rep.*, vol. 7, pp. 55–61, Oct. 2021, doi: 10.1016/j.egy.2021.09.040.
- [24] J.-P. Jimenez-Navarro, K. Kavvadias, F. Filippidou, M. Pavičević, and S. Quoilin, "Coupling the heating and power sectors: The role of centralised combined heat and power plants and district heat in a European decarbonised power system," *Appl. Energy*, vol. 270, p. 115134, Jul. 2020, doi: 10.1016/j.apenergy.2020.115134.
- [25] E. Trømborg, M. Havskjold, T. F. Bolkesjø, J. G. Kirkerud, and Å. G. Tveten, "Flexible use of electricity in heat-only district heating plants," *Int. J. Sustain. Energy Plan. Manag.*, pp. 29-46 Pages, Mar. 2017, doi: 10.5278/IJSEPM.2017.12.4.
- [26] B. V. Mathiesen *et al.*, "Smart Energy Systems for coherent 100% renewable energy and transport solutions," *Appl. Energy*, vol. 145, pp. 139–154, May 2015, doi: 10.1016/j.apenergy.2015.01.075.
- [27] P. A. Østergaard and H. Lund, "A renewable energy system in Frederikshavn using low-temperature geothermal energy for district heating," *Appl. Energy*, vol. 88, no. 2, pp. 479–487, Feb. 2011, doi: 10.1016/j.apenergy.2010.03.018.
- [28] T. Nussbaumer, S. Thalmann, A. Jenni, and J. Ködel, "Handbook on Planning of District Heating Networks." 2020.
- [29] BDEW, VKU, and GEODE, "Leitfaden. Abwicklung von Standardlastprofilen Gas." 2022.

- [30] A. Kallert, R. Egelkamp, U. Bader, D. Münnich, L. Staudacher, and H. Doderer, “A multi-valent supply concept: 4th Generation District Heating in Moosburg an der Isar,” *Energy Rep.*, vol. 7, pp. 110–118, Oct. 2021, doi: 10.1016/j.egy.2021.09.032.
- [31] “Energieatlas Bayern,” *energieatlas.bayern.de*. <http://www.energieatlas.bayern.de> (accessed Apr. 06, 2023).
- [32] “Uni-Kassel Downloads.” <https://www.uni-kassel.de/maschinenbau/en/institute/thermische-energie-technik/fachgebiete/solar-und-anlagentechnik/downloads> (accessed Apr. 25, 2023).
- [33] LOGSTOR, “Logstor Fernwaermerohre Produktkatalog.” 2020.
- [34] “Wilo-Select 4.” Accessed: Mar. 08, 2023. [Online]. Available: <https://www.wilo-select.com/Region.aspx>
- [35] “HiRef S.p.A. Website,” *HiRef*. <https://hiref.it/hiref.it/> (accessed Jun. 06, 2023).
- [36] “Upper groundwater layer: Current data HEINRICHSHEIM 34.02.” <https://www.gkd.bayern.de/en/groundwater/upper-layer/bayern/heinrichsheim-34-02-11664/current-values> (accessed Apr. 06, 2023).
- [37] “Temperature of springs: Chart of year Karstquelle Ettling.” <https://www.gkd.bayern.de/en/groundwater/temperature-of-springs/kelheim/karstquelle-ettling-11507/year-figures?zr=jahr&dir=prev&start=01.01.2023> (accessed Apr. 06, 2023).
- [38] “Flow of well: Current data Karstquelle Ettling.” <https://www.gkd.bayern.de/en/groundwater/flow-of-springs/kelheim/karstquelle-ettling-11507/current-values> (accessed Apr. 06, 2023).
- [39] C. S. Blázquez, V. Verda, I. M. Nieto, A. F. Martín, and D. González-Aguilera, “Analysis and optimization of the design parameters of a district groundwater heat pump system in Turin, Italy,” *Renew. Energy*, vol. 149, pp. 374–383, Apr. 2020, doi: 10.1016/j.renene.2019.12.074.
- [40] J. Bonin, *Heat pump planning handbook*. London, New York: Routledge, 2015.
- [41] C. Fünfgeld and R. Tiedemann, “Repräsentative VDEW-Lastprofile.” 2000.
- [42] “Stromverbrauch vergleichen: Stromspiegel.” https://www.co2online.de/energie-sparen/strom-sparen/strom-sparen-stromspartipps/stromspiegel-stromverbrauch-vergleichen/?gclid=Cj0KCQjw4NujBhC5ARIsAF4Iv6crM6_-YHTFw-AqPAMjr9qky7Sco0IOzSS5u_vUWYt8G5Dy4uoltxMaAqKHEALw_wcB (accessed Jun. 22, 2023).
- [43] “Produkte für Nah- und Fernwärme | Enerpipe GmbH.” <https://www.enerpipe.de/produkte> (accessed Jun. 25, 2023).
- [44] Deutsches Institut für Normung e.V., “DIN EN 15450. Heizungsanlagen in Gebäuden – Planung von Heizungsanlagen mit Wärmepumpen.” 2007.
- [45] OCHSNER Wärmepumpen GmbH, “Bedienungs- und Installationsanleitung”.
- [46] “MATLAB Documentation - MathWorks Italia.” <https://it.mathworks.com/help/matlab/> (accessed Nov. 14, 2022).

- [47] “Simulink Documentation - MathWorks Italia.” <https://it.mathworks.com/help/simulink/> (accessed Nov. 14, 2022).
- [48] G. Schweiger *et al.*, “District energy systems: Modelling paradigms and general-purpose tools,” *Energy*, vol. 164, pp. 1326–1340, Dec. 2018, doi: 10.1016/j.energy.2018.08.193.
- [49] “CARNOT Toolbox des Solar-Institut Jülich,” *FH Aachen*. <https://www.fh-aachen.de/forschung/institute/sij/carnot> (accessed Jun. 26, 2023).
- [50] “CARNOT manual.” https://www.fh-aachen.de/fileadmin/ins/ins_sij/pdfs/Manual.html (accessed Mar. 09, 2023).
- [51] N. Abdurahmanovic, “Comparison and modification of the heat pump model”.
- [52] S. Hirzel, “ENERGY EXPLAINED - Primary energy factors”.
- [53] Deutsches Institut für Normung e.V. (Hrsg), “DIN V 18599-1. Energetische XVI Bewertung von Gebäuden - Berechnung des Nutz-, End- und Primärenergiebedarfs für Heizung, Kühlung, Lüftung, Trinkwarmwasser und Beleuchtung.” Deutsche Norm. Beuth Verlag, Berlin, 2018.
- [54] M. Gruber, “Gutachten. Bestimmung des Primärenergiefaktors für das Wärmenetz „Neuburg a. d. Donau“ der Stadtwerke Neuburg a. d. Donau.” 2022.
- [55] Google Maps, “Neuburg an der Donau · 86633,” *Neuburg an der Donau · 86633*. <https://www.google.de/maps/place/86633+Neuburg+an+der+Donau/@48.7350072,11.2203043,994m/data=!3m1!1e3!4m6!3m5!1s0x479ee3846376818f:0x41e48add78ba530!8m2!3d48.7302674!4d11.1887693!16zL20vMDc5ajA2!5m1!1e4?entry=ttu> (accessed Jun. 26, 2023).
- [56] Deutsche Umwelthilfe, “Promoting Renewable District Heating Seven Policy Recommendations.” 2021.

Appendix

A.1 Heat load and heating demand

Table A.1 Heat load and heating demand for the buildings in the Heckenweg district.

Nr.	Area	Nr. in the area	Type	Heat load [kW]	Heating demand [kWh/year]
1	Heckenweg	1	SFH	16.90	27,230
2	Heckenweg	2	SFH	13.50	21,784
3	Heckenweg	3	SFH	13.40	21,619
4	Heckenweg	4	DFH	9.20	14,915
5	Heckenweg	6	DFH	9.20	14,915
6	Heckenweg	7	DFH	14.70	24,867
7	Heckenweg	9	DFH	12.80	21,652
8	Heckenweg	11	SFH	11.80	18,978
9	Heckenweg	12	SFH	7.80	12,670
10	Heckenweg	13_1	DFH	9.40	15,226
11	Heckenweg	13_2	DFH	8.30	13,517
12	Heckenweg	15	SFH	10.80	17,493
13	Heckenweg	16	DFH	8.80	14,294
14	Heckenweg	17	SFH	10.60	17,163
15	Heckenweg	18	DFH	8.80	14,294
16	Heckenweg	19	SFH	17.40	28,055
17	Heckenweg	20	DFH	8.20	13,361
18	Heckenweg	21_1	SFH	8.70	15,086
19	Heckenweg	21_2	SFH	8.80	15,234
20	Heckenweg	22	DFH	8.20	13,361
21	Heckenweg	23	SFH	12.80	20,629
22	Heckenweg	24	DFH	8.80	14,294
23	Heckenweg	25	SFH	8.90	14,358
24	Heckenweg	26	DFH	8.80	14,294
25	Heckenweg	28	DFH	8.20	13,361
26	Heckenweg	30	DFH	8.20	13,361
27	Heckenweg	32	SFH	11.20	17,988
28	Heinrichsheimstraße	7	SFH	22.60	38,027
29	Heinrichsheimstraße	9	SFH	28.60	41,208
30	Heinrichsheimstraße	11_1	DFH	12.10	20,580
31	Heinrichsheimstraße	11_2	DFH	7.60	12,429
32	Heinrichsheimstraße	13	SFH	15.50	24,919
33	Heinrichsheimstraße	15	SFH	21.20	30,507
34	Heinrichsheimstraße	17_1	DFH	14.30	20,500

35	Heinrichsheimstraße	17_2	DFH	14.10	20,269
36	Heinrichsheimstraße	19_1	DFH	16.40	23,494
37	Heinrichsheimstraße	19_2	DFH	14.00	20,039
38	Heinrichsheimstraße	21	DFH	10.70	13,579
39	Heinrichsheimstraße	22	SFH	17.90	23,237
40	Heinrichsheimstraße	23	DFH	10.70	13,579
41	Heinrichsheimstraße	24	SFH	14.70	23,764
42	Heinrichsheimstraße	25	SFH	29.50	38,259
43	Heinrichsheimstraße	26	DFH	16.40	20,787
44	Heinrichsheimstraße	27	SFH	8.50	10,717
45	Heinrichsheimstraße	28	DFH	28.10	35,540
46	Heinrichsheimstraße	29	SFH	16.20	20,583
47	Heinrichsheimstraße	30	SFH	14.80	24,118
48	Heinrichsheimstraße	31	SFH	23.50	30,513
49	Heinrichsheimstraße	32	SFH	18.80	24,411
50	Heinrichsheimstraße	33	SFH	11.50	18,483
51	Heinrichsheimstraße	34	SFH	26.00	43,719
52	Heinrichsheimstraße	38	SFH	14.50	18,372
53	Heinrichsheimstraße	40	SFH	14.50	18,372
54	Heinrichsheimstraße	42	SFH	10.30	13,098
55	Heinrichsheimstraße	44	SFH	15.30	19,393
56	Heinrichsheimstraße	46	SFH	13.20	16,671
57	Heinrichsheimstraße	48	SFH	29.70	38,493
58	New development	1	SFH	5.40	6,300
59	New development	2	SFH	5.13	5,985
60	New development	3	SFH	4.86	5,665
61	New development	4	SFH	6.28	7,327
62	New development	5	SFH	5.43	6,339
63	New development	6	SFH	5.94	6,930
64	New development	7	SFH	6.08	7,088
65	New development	8	SFH	5.06	5,906
66	New development	9	SFH	6.14	7,166
67	New development	10 (a and b)	DFH	8.86	10,336
68	New development	11 (a and b)	DFH	8.86	10,336
69	New development	12 (a and b)	DFH	8.86	10,336
70	New development	13 (a and b)	DFH	7.21	8,416
71	New development	14 (a and b)	DFH	11.14	12,994
72	New development	15 (a and b)	DFH	10.69	12,469
73	New development	16 (a to c)	RH	19.02	22,188
74	New development	17 (a to d)	RH	24.84	28,980
75	New development	18 (a to b)	DFH	9.84	11,484
76	New development	19	SFH	14.51	16,923

77	New development	20 (a to h)	RH	59.06	68,906
78	New development	21	SFH	13.97	16,301
79	New development	22 (a to r)	MFH	271.48	316,722
80	New development	23 (a and b)	MFH	38.41	44,809
81	New development	24 (a and b)	MFH	39.23	45,773
82	New development	25 (a and b)	MFH	38.39	44,789
			Total	1430.09	1,922,127

A.2 Other parameters for the buildings

Table A.2 Other considered parameters for the buildings in the Heckenweg district.

Nr.	DHW requirement [L/day]	Installed PV [kWp]	Electricity demand [kWh/year]
1	80.5	14	4,200
2	80.5	12	4,200
3	80.5	11	4,200
4	46	8	4,200
5	46	8	4,200
6	46	10	4,200
7	46	9	4,200
8	80.5	10	4,200
9	80.5	10	4,200
10	46	9	4,200
11	46	8	4,200
12	80.5	9	4,200
13	46	8	4,200
14	80.5	9	4,200
15	46	8	4,200
16	80.5	15	4,200
17	46	8	4,200
18	80.5	9	4,200
19	80.5	9	4,200
20	46	8	4,200
21	80.5	11	4,200
22	46	8	4,200
23	80.5	8	4,200
24	46	8	4,200
25	46	8	4,200
26	46	8	4,200

27	80.5	10	4,200
28	80.5	15	4,200
29	80.5	16	4,200
30	46	8	4,200
31	46	7	4,200
32	80.5	13	4,200
33	80.5	12	4,200
34	46	8	4,200
35	46	8	4,200
36	46	9	4,200
37	46	8	4,200
38	46	7	4,200
39	80.5	9	4,200
40	46	7	4,200
41	80.5	13	4,200
42	80.5	14	4,200
43	46	11	4,200
44	80.5	7	4,200
45	46	19	4,200
46	80.5	11	4,200
47	80.5	19	4,200
48	80.5	11	4,200
49	80.5	9	4,200
50	80.5	10	4,200
51	80.5	17	4,200
52	80.5	9	4,200
53	80.5	9	4,200
54	80.5	7	4,200
55	80.5	10	4,200
56	80.5	9	4,200
57	80.5	14	4,200
58	80.5	10	4,200
59	80.5	10	4,200
60	80.5	9	4,200
61	80.5	12	4,200
62	80.5	11	4,200
63	80.5	12	4,200
64	80.5	12	4,200
65	80.5	10	4,200
66	80.5	12	4,200
67	92	14	4,200
68	92	14	4,200

69	92	14	4,200
70	92	11	4,200
71	92	17	4,200
72	92	17	4,200
73	138	25	20,075
74	184	32	25,550
75	92	15	4,200
76	80.5	19	4,200
77	368	76	60,226
78	80.5	18	14,600
79	8682.5	340	275,576
80	966	50	38,125
81	1012	51	40,150
82	966	50	38,325
Total	17606.5	1440	823,427